Title
Study of Ubiquitinating Enzymes Essential for Cell Proliferation

Author
Jin, Lingyan

Publication Date
2012

Peer reviewed|Thesis/dissertation

Study of Ubiquitinating Enzymes Essential for Cell Proliferation

By

Lingyan Jin

A dissertation submitted in partial satisfaction of the

requirements for the degree of

Doctor of Philosophy

in

Molecular and Cell Biology

in the

Graduate Division

of the

University of California, Berkeley

Committee in Charge:

Professor Michael Rape, Chair
Professor Robert Tjian
Professor Eva Nogales
Professor Irina Conboy

Spring 2012

The dissertation of Lingyan Jin, titled Study of Ubiquitinating Enzymes Essential for Cell Proliferation,
is approved:

Chair _____ Date _____

_____ Date _____

_____ Date _____

_____ Date _____

University of California, Berkeley

Study of Ubiquitinating Enzymes Essential for Cell Proliferation

by

Lingyan Jin

Abstract

Study of Ubiquitinating Enzymes Essential for Cell Proliferation

by

Lingyan Jin

Doctor of Philosophy in Molecular and Cell Biology

University of California, Berkeley

Professor Michael Rape, Chair

Ubiquitination is a form of post-translational modification of proteins, in which the 76-residue ubiquitin polypeptide is conjugated to the lysine residues of either the substrate protein or the preceding ubiquitin molecule. Ubiquitination requires the sequential action of three types of ubiquitin enzymes: the ubiquitin activating enzyme (E1), the conjugating enzyme (E2) and the ligase (E3). In human genome, there are two different E1s, ~40 E2s and more than 600 E3s. Ubiquitination regulates a variety of cellular processes, including cell cycle progression, induction of inflammatory response, or intracellular protein trafficking. The anaphase-promoting complex/cyclosome (APC/C) and the SCF are two important E3 ligases regulating cell cycle progression. Understanding how they recognize their substrates and how their enzymatic activity is regulated will provide valuable clues for inhibiting unchecked cell proliferation such as in cancer. The objective of this dissertation is twofold: 1) Chapter 1: understanding how APC/C forms ubiquitin chains on its substrates. We found that APC/C preferentially uses lysine11 of ubiquitin to assemble ubiquitin chains on its substrates. By recognizing the same motif present in both the substrates and ubiquitin, APC/C switches from initial modification of the substrate to processive chain elongation, leading to the rapid turnover of its substrates. 2) Chapter 2 to 5: identifying $Cul3^{Klhl12}$, a structural relative of SCF, as an essential ubiquitin ligase in embryonic stem cells (ESCs). In an siRNA screen, we found that $Cul3^{Klhl12}$ affects cell adhesion and proliferation of ES cells by regulating COPII-mediated protein trafficking. $Cul3^{Klhl12}$ ubiquitinates Sec31A, a coat protein of COPII vesicles, and causes the enlargement of the vesicles. This enables the COPII-dependent transport and proper deposition of collagen, a major component of extracellular matrix (ECM).

To Mother, Farther, Hanshen and George

TABLE OF CONTENTS

LIST OF FIGURES

Note: Images in Chapter One are first published in Cell. 2008 May 16;133(4):653-65. Images in Chapter Two to Five are first published in Nature. 2012 Feb 22;482(7386):495-500.

ACKNOWLEDGEMENTS

First and foremost I would like to express my sincerest gratitude to my PhD advisor, Professor Michael Rape, for his guidance and support throughout the last five and half years. Michael is an encouraging and supportive mentor. He set an example for me to be an inspiring and hardworking scientist. He also gave me the freedom to explore a risky project and provided necessary support all the way towards the completion of my PhD thesis. I am honored to be a part of his lab and believe that these years of scientific training will definitely benefit my future career.

I am deeply grateful to Tang fellowship for supporting me to study at UC Berkeley. I appreciate the generosity and kindness of Nadine Tang and Leslie Tang, and will be glad to share any good news with them.

I would like to thank my thesis committee members: Professor Robert Tjian, Professor Eva Nogales, and Professor Irina Conboy for their helpful advice on my thesis. I appreciate Professor Tjian and Professor Nogales for giving me the opportunity to rotate in their labs.

I would like to thank the past and present members of Rape Lab for all their help. I want to especially thank Kate and Adam for their collaboration on the projects. Our lab alumni, Christine, Sudeep and Christina, also helped a lot on the projects. I will definitely miss the time with my labmates, who have added a lot of fun to my life in graduate school: Ling and Zaiming for being my 'lunchdates', Kate and Adam for helping me move my apartment, and all my labmates for their precious gifts for my baby.

I appreciate members of the Schekman Lab for their generosity and inclusiveness. I especially appreciate the support and advice from Professor Randy Schekman. Kanika and Amita, my collaborators, contributed tremendously to the completion of the project. I want to thank Bob, Yusong, Regina, Sean, Soomin, Lillian, Zhiliang, Zhe and Yick for sharing reagents and for useful discussion on the project. Ann Fischer and Michelle Richner provided a lot of support in tissue culture.

I dedicate this thesis to my beloved family. I am proud to have the most wonderful parents, whose unfailing love is the eternal sunshine in my heart, guiding me through all the adversity and giving me hope and courage. I am lucky to have Hanshen, my loving husband and best friend, with whom I can share all my happiness and unhappiness. I appreciate his company. Last but not least, I want to thank my lovely son George for bringing endless joy to my life. Nothing can be compared with seeing him growing up.

Chapter One

Identification of Novel Ubiquitin Chains Formed by Anaphase-Promoting Complex (APC/C)

1.1 Introduction

The anaphase-promoting complex/cyclosome (APC/C) is a multi-subunit RING-E3 essential for cell proliferation in all eukaryotes. The APC/C is so named as it was first discovered to be required for the progression from metaphase to anaphase during mitosis by promoting the ubiquitination and degradation of Cyclin B1 and Securin. Its substrate spectrum, however, extends far beyond the regulators for anaphase progression. It also regulates the dynamics of spindle assembly by ubiquitinating key spindle assembly factors (SAFs) and maintains the G1 state by degrading geminin, Cyclin A and Polo kinase (Song, et. al., 2010). The APC/C has 13 constituent proteins with a total molecular mass of 1.1MDa. The catalytic activity is provided by RING-finger protein Apc11 which is anchored to Apc2, a scaffold protein in APC/C with additional structural proteins Cdc27, Cdc16, Cdc23, Cdc26, Apc1, Apc4, Apc5, Apc9, APC10 (Doc1), Apc13 and Mnd2. In addition, two WD40-domain-containing co-activators Cdc20 and Cdh1 associate with APC/C core domain as substrate recognition factors (Herzog, et. al., 2009; Scheiber, et. al., 2010). In vivo, Cdc20 is the binding partner for APC/C in metaphase, which is degraded by autoubiquitination and replaced by Cdh1 soon after mitosis. Both Cdc20 and Cdh1 have similar substrate specificity, proteins with characteristic D-box and KEN box. Recent work from our lab has revealed an additional TEK box about 20aa downstream of D-box is required for the proper recognition by APC/C (Jin, et. al., 2008; Williamson, et. al., 2011). The activity of APC/C is highly regulated through cell cycle. The spindle checkpoint proteins Mad2 and BubR1 bind to APC/C^{cdc20} and prevent anaphase progression until all kinetochores are properly attached to the microtubules. Cdc20 gets quickly auto-ubiquitinated, leading to the release of Mad2 and BubR1 and full activation of APC/C (Reddy, et. al., 2007). During late G1, APC/C is deactivated by degradation of its specific E2 UbcH10 and UBE2S (Rape, et. al., 2004; Williamson, et. al., 2009).

Despite its essential roles in many stages of cell cycle, little is known about how this 1MDa huge E3 ligase complex efficiently modifies lysine residues both in substrates and in the ubiquitin molecules of a growing chain. To gain insight into the mechanism of ubiquitin chain formation, we determined the topology and the mechanism of assembly for the ubiquitin chains mediating the mitotic functions of the APC/C. We find that the APC/C promotes the inactivation of the spindle checkpoint and proteasomal degradation of cell cycle regulators by assembling K11-linked ubiquitin chains. The efficient formation of K11-linked chains by the APC depends on a charged surface of ubiquitin, which is centered around K11 and referred to as the TEK-box. Adam Williamson in our lab found that homologous TEK-box sequences are also present in APC-substrates, such as securin, where they facilitate the APC-dependent transfer of the first ubiquitin to a substrate lysine residue. By recognizing similar sequence motifs in ubiquitin and substrates, the APC/C is able to catalyze the formation of substrate-linked ubiquitin chains with high specificity and efficiency required for cell cycle control.

1.2 Results

1.2.1 K11-linked Ubiquitin Chains Support the Degradation of APC/C Substrates

Previous study showed that the Xenopus APC/C can modify K11, K48 and K63 of ubiquitin in vitro (Kirkpatrick et al., 2006). However, the topologies of the ubiquitin chains that mediate the disassembly of spindle checkpoint complexes or the proteasomal degradation of cell cycle regulators were not identified. To address this fundamental question, we employed two sets of ubiquitin mutants in in-vitro assays that recapitulate APC-dependent complex disassembly and protein degradation, respectively. In one set of mutants, one of the seven lysine residues of ubiquitin was mutated to arginine, such as ubiquitin-K48R (referred to as ubi-R48). These mutants enabled us to determine whether a specific lysine residue is required for complex disassembly or protein degradation. A complementary set of ubiquitin mutants had all lysine residues mutated to arginine except for one, such as ubiquitin with K48 as its only lysine (ubi-K48). These single-lysine mutants allowed us to assess whether chain formation through a specific lysine residue of ubiquitin is sufficient to mediate APC-dependent functions.

We first assayed the ubiquitin mutants for their capacity to support the degradation of a mitotic APC/C substrate, cyclin B1. Addition of UbcH10 and $p31^{comet}$ to extracts of mitotic cells with an activated spindle checkpoint (CP extracts) triggers the APC/C-dependent disassembly of Cdc20/Mad2 complexes (Reddy et al., 2007; Stegmeier et al., 2007). This leads to full activation of APC/C^{Cdc20} and, consequently, cyclin B1 ubiquitination and degradation. As reported previously, cyclin B1 is efficiently degraded in UbcH10/$p31^{comet}$-treated CP extracts containing wild-type (WT) ubiquitin (Fig. 1-1A). Strikingly, cyclin B1 is also turned over in a proteasome-dependent manner, when CP extracts are supplemented with a ubiquitin mutant that has K11 as its only lysine (ubi-K11; Fig. 1-1A and 1-1B). In contrast, mutation of K11 of ubiquitin (ubi-R11) interferes with cyclin B1 degradation (Figure 1-1C). No single-lysine ubiquitin mutant other than ubi-K11, including ubi-K48, supports degradation of cyclin B1, while no mutation other than that of K11 stabilizes cyclin B1. These results suggest that in CP extracts APC/C^{Cdc20} achieves cyclin B1 degradation by decorating it with K11-linked chains.

In early mitosis, the APC is activated by Cdc20, which during anaphase is replaced by a homologous co-activator, Cdh1. APC^{Cdh1} remains active in G1, until it is inhibited by degradation of its E2 UbcH10, cyclin A-dependent phosphorylation of Cdh1, and binding of an inhibitor, Emi1. To determine whether the nature of the co-activator or the cell cycle stage influence the topology of APC-dependent ubiquitin chains, we employed the ubiquitin mutants in degradation assays using G1-extracts. Consistent with our previous experiments in mitotic extracts, the APC-substrate securin was rapidly degraded in G1-extracts supplemented with ubi-K11, but it was stabilized if K11 of ubiquitin was mutated, such as in ubi-R11 (Fig. 1-1D). No single-lysine mutant other than ubi-K11 fully supported the degradation of securin in G1-extracts. Together, these findings provide strong evidence that the APC targets substrates for degradation by assembling K11-linked ubiquitin chains in both mitosis and G1 phase.

To determine the importance of K11-linked chains in mediating APC/C functions in vivo, we overexpressed ubi-R11 in human cells. The overexpression of ubi-R11 in human 293T cells impedes the Cdh1-dependent degradation of the APC/C substrates geminin, Plk1, and securin Δ

D (Fig. 1-1E), indicating that K11-linked ubiquitin chains are also required for APC/C activity in vivo.

1.2.2 APC/C Substrates Modified with K11-linked Ubiquitin Chains are Recognized by Proteasomal Receptors

To confirm that the degradation of APC/C substrates in the presence of ubi-K11 is due to the direct assembly of K11-linked ubiquitin chains on APC/C substrates, we set up an in-vitro ubiquitination assay of APC/C substrates using affinity-purified APC/C complex from Hela G1 extract. Consistant with our observation in degradation assay, APC/C^{Cdh1} and its specific E2 UbcH10 form long ubiquitin chains on its substrate Cyclin A, only in the presence of ubi-K11 but not with other single-lysine mutants (Fig. 1-2A). The same strong preference of linkage specificity is also observed with other APC/C substrates, including UbcH10 itself (data not shown). In contrast to UbcH10, UbcH5c can use ubi-K11, ubi-K48 and ubi-K63 to assemble ubiquitin chains on APC/C substrates (Fig. 1-2B). However, UbcH5c-mediated chain formation is not able to cause degradation of APC/C substrates, indicating that the K11-specific ubiquitin chains are much more efficient at targeting APC/C substrates for degradation than branched ubiquitin chains (Fig. 1-2C).

Proteins modified with ubiquitin chains are targeted for degradation by proteasome through proteasomal substrate receptors. These receptors selectively recognize ubiquitin chains of certain topology and have higher affinity towards longer ubiquitin chains than single or double ubiquitins. To test whether K11-linked ubiquitin chains can be efficiently recognized by proteasomal substrate receptors, we assembled K11 chains on APC/C substrate using in-vitro ubiquitination assay and mix it with proteasomal substrate receptor Rad23 immobilized on GST beads. We found that K11-linked ubiquitin chains can be recognized by Rad23 as efficiently as wildtype ubiquitin chains (Fig. 1-2D). Although APC/C and UbcH10 are also able to assemble ubiquitin chains without K11 by using ubi-R11, these branched ubiquitin chains are poor targeting signals for Rad23. In addition, K11-linked ubiquitin chains can also be recognized by other proteasomal substrate receptors like S5a and Plic2 (Fig. 1-2E). Consistant with previous report, only the longer ubiquitin chains with K11 linkage but not short ubiquitin chains nor the substrate itself can bind the proteasomal receptors.

1.2.3 Identification of a Surface on Ubiquitin Important for the Assembly of K11-linked Ubiquitin Chains

Formation of K11-linked chains by the APC/C requires the alignment of K11 in the acceptor ubiquitin relative to the active site of UbcH10. To identify residues in ubiquitin that help present K11, we mutated surface-exposed amino acids to alanine and monitored the capacity of these mutants to support APC/C activity in extracts. Out of a total of 17 ubiquitin mutants, substituting K6, L8, T9, E34, and I36 with alanine strongly stabilizes securin in extracts (Fig. 1-3A). Accordingly, overexpression of ubi-K6A and ubi-L8A in 293T cells interferes with the degradation of the APC/C^{Cdh1} substrate securinΔD to a similar extent as overexpression of

ubi-R11 (Fig. 1-3B). Overexpression of ubi-L8A reduced the modification of securin also in cells (Figure 1-3C). Interestingly, if the positive charge at position 6 is maintained, as in ubi-R6, neither degradation nor ubiquitination of APC/C substrates is strongly affected (Fig. 1-1D, Fig. 1-2A). This suggests that K6 contributes to binding but is unlikely to be ubiquitinated itself. These experiments identify the ubiquitin residues K6, L8, T9, E34, and I36 to be required for the efficient formation of K11-linked chains by the APC/C and UbcH10. Importantly, these residues form a cluster surrounding K11, which we refer to as the TEK-box of ubiquitin (Fig. 1-3D).

In contrast to mutating the TEK-box, altering several other positions of ubiquitin does not affect ubiquitination or degradation of APC/C substrates. These include residues shown to support the formation of K29 linkages by a HECT-E3 (E16A/E18A), the formation of K48 and K63 linkages by several E3s (I44A; K48R; Y59A; K63A/E64A), and ubiquitin recognition (I44A, D58A). Moreover, when UbcH5c is used as E2, mutations in the TEK-box inhibit the APC/C-dependent chain formation less severely (data not shown). Only ubi-L8A, and to a lesser extent ubi-I36A, are deficient in supporting chain formation by APC/C^{Cdh1} and UbcH5c.

1.2.4 Ubiquitin Deficient of K11 Causes Cell Cycle Arrest During Early Embryogenesis of *Xenopus tropicalis*

The identification of ubiquitin K11 as the preferred ubiquitination site by human APC/C is interesting as yeast APC/C uses the canonical K48 to assemble ubiquitin chains. The switch of linkage specificity could be partly due to the fact that yeast lacks a human homolog of UbcH10. Instead, the yeast APC/C uses Ubc4, a human homolog of UbcH5, as its endogenous E2. The diversification of ubiquitin chains with different linkages as targeting signals for proteasomal degradation may confer evolutionary advantages to higher eukaryotes, in which the control of cell proliferation and differentiation is much more complicated than yeast.

To determine the importance of K11-linked ubiquitin chains during early development of higher eukaryotes, we injected ubiquitin mutants into one cell of the fertilized Xenopus egg at the two-cell stage. When injected with wildtype ubiquitin, both sides of the embryo divided normally and the embryo developed into viable tadpole (Fig. 1-4A, Fig. 1-4B). However, the injection of ubiquitin protein with K11 mutated to arginine significantly slowed down cell division on the side of injection, and very few of the injected embryos grew into tadpoles. Considering the abundance of endogenous wildtype ubiquitin, the phenotype is very dramatic, underlying the importance of K11-linked ubiquitin chains during embryogenesis. Similarly, an obvious cell cycle arrest was observed when the dominant negative form of UbcH10 was injected.

1.3 Discussion

The modification of proteins with ubiquitin chains is a crucial regulatory event in eukaryotes. Ubiquitin chains formed by different lysines have distinct cellular functions. Ubiquitin chains linked through K48 are targeting signals for proteasomal degradation, whereas ubiquitin chains with K63 linkage are non-degradative, leading to protein complex remodeling

during signal transduction. Our work has shown for the first time that K11-linked ubiquitin chains formed by human APC/C target its substrates to degradation. Katherine Wickliffe and Adam Williamson in our lab identified a novel APC/C associated E2, UBE2S, which exclusively elongates ubiquitin chain through K11 after chain nucleation of APC/C substrates by UbcH10 (Williamson, et. al., 2009; Wickliffe, et. al., 2011).

Why do human APC/C and its E2s preferentially use K11 instead of the canonical K48 for chain formation? One possibility could be the differential binding ability of different ubiquitin chains towards various ubiquitin binding proteins. Structural analyses of ubiquitin dimers and tetramers have shown that ubiquitin chains with different linkages adopt distinct conformations. K63-linked ubiquitin chain adopts an 'open' conformation with each ubiquitin molecule freely accessible in solvent (Varadan et. al., 2004). Upon binding to Rad23, the hydrophobic patch of each ubiquitin binds with one UBA domain achieving a molar ratio of 2:1 UBA:Ub_2. K11- and K48-linked ubiquitin chains both have 'closed' conformations but with distinct topology. The adjacent ubiquitin molecules of K48 dimers are tightly 'locked' to each other through the hydrophobic patch of Leu8, Ile44 and Val70 (Varadan et. al., 2005). The binding to UBA domain of Rad23 requires the opening of K48 dimers and one single UBA is inserted in between the adjacent ubiquitin molecules. It has been shown that K48-linked ubiquitin dimers and tetramers have higher affinity with UBA domain compared with K63-linked dimers and tetramers, respectively. It is likely that the principle basis against K63 chain is the entropic cost of immobilizing the flexible chain upon binding. On the other hand, some ubiquitin binding proteins like TAB2 and TAB3 which activate NF κ B pathway specifically interact with K63- but not K48-linked chains (Sato, et. al., 2009). A recent study of K11-linked ubiquitin dimer showed that the interaction between adjacent ubiquitin molecules is electrostatic (Bremm, et. al., 2010), with the hydrophobic patch exposed in the solvent. How the K11-linked ubiquitin chain is recognized by proteasomal adaptors like Rad23 and subsequently targeted to degradation remains to be understood. It will also be interesting to determine the relative binding affinity of different ubiquitin chains with various ubiquitin binding proteins. Finding the K11 chain-specific binding partners will provide clues about additional physiological functions of this novel chain type.

Another layer of regulation may come from the linkage specificity of de-ubiquitination enzymes (DUBs). Cezanne, an OTU domain containing DUB, disassembles K11-linked ubiquitin chains with high specificity. It is not clear yet whether Cezanne or other K11-specific DUBs regulate the ubiquitination and degradation of APC/C substrates in cells.

1.4 Material and Methods

Plasmids and Antibodies

Human securin, geminin, cyclin A, cyclin B1, Plk1, and Cdc20 were cloned into pCS2 for IVT/T and into pET28 for purification. Rad23, S5a, and hPlic2 were cloned into pGEX4T1 for purification and into pCS2-HA for immunoprecipitations. His6-tagged ubiquitin was cloned into pET28 for purification. Ubiquitin was cloned into pCS2 for expression in cells. Antibodies were purchased for detection of Cdc27, Mad2, securin, geminin, and cyclin B1 (Santa Cruz), Plk1 (Upstate), securin (MBL), and b-actin (Abcam).

Degradation Assays

Concentrated extracts of HeLa S3 cells in mitosis and G1 were made as described (Williamson, et. al., 2009). The mitotic extract was supplemented with UbcH10 (5 μM) and $p31^{comet}$ (1 μM) to activate the APC/C. Recombinant ubiquitin or mutants (～50 μM) were added. Reactions were analyzed for degradation of endogenous cyclin B1 by western blotting. The G1 extract was supplemented with recombinant ubiquitin mutants (～50 μM) and radiolabeled securin mutants. The radiolabeled substrates were synthesized by IVT/T using TnT-system (Promega). Reactions were analyzed for substrate degradation by autoradiography.

In Vitro Ubiquitination Reactions

In vitro ubiquitination reactions were performed as described (Rape et al., 2006). The APC/C was purified from 1.5 ml G1 extracts using 75 μl monoclonal αCdc27 antibodies and 100 μl Protein G-agarose (Roche). Washed beads were incubated with 50 nM E1, 100 nM E2, 1 mg/ml ubiquitin, energy mix (20 mM ATP, 15 mM creatine phosphate, creatine phosphokinase), 1 mM DTT at 23℃. Reactions were analyzed by autoradiography.

Purification of Ubiquitin Conjugates from Cells

293T cells expressing securin and His-ubiquitin mutants were lysed in 6M GdHCl and purified by NiNTA agarose. Ubiquitinated securin was detected by western blotting using securin antibodies. For binding assays, 293T cells expressing securin, ubi, and HARad23 were lysed by freeze/thaw. Cleared lysates were added to anti-HA agarose(Roche), incubated at 4℃, and probed for copurifying securin by western blotting.

In Vivo Degradation Assays

Most in vivo degradation assays were performed in 293T cells. APC/C substratesand Cdh1 were coexpressed for 20–24 hr in the presence of His-ubiquitin or respective mutants. Cells were lysed and probed for the levels of the APC/C substrates by western blotting.

In Vitro Fertilization and Injection of Xenopus tropicalis Embryos

Females were primed with 10 U hGC and males boosted with 100 U hGC. The next day, females were boosted with 100 U hGC. Males were anesthetized in 0.05% benzocaine and testes were isolated. Sperm and eggs were gently mixed. Thirty minutes after activation, media are changed to 3% cysteine for 15 min and then to 1/9 MR solution containing 3% ficoll. One cell of a two cell stage embryo is injected with 32 ng of protein premixed with minored tracer. Injected embryos were selected by fluorescence, and the phenotypes at different developmental stages were analyzed and quantified.

Fig. 1-1: K-11 linked ubiquitin chains mediate the degradation of APC/C substrates

(A) K11-linked chains are sufficient for degradation of cyclin B1 in mitotic extracts. CP extracts were supplemented with WT-ubi or single-lysine mutants. The APC/C was activated by addition of UbcH10 and $p31^{comet}$, and degradation of cyclin B1 was monitored by western blotting.

(B) Degradation of APC/C substrates by K11-linked chains is proteasome dependent. Degradation of cyclin B1 in CP extracts was triggered by addition of p31comet/UbcH10 in the presence of WT-ubi or ubi-K11. The proteasome inhibitor MG132 was added when indicated.

(C) K11 is required for rapid degradation of cyclin B1 in mitotic extracts. CP extracts were supplemented with ubiquitin mutants and treated as described above. Degradation of cyclin B1 was monitored by western blotting.

(D) K11 linkages are required for full activity of APC/C^{Cdh1} in G1. The degradation of radiolabeled securin was monitored by autoradiography in G1 extracts in the presence of ubiquitin mutants.

(E) K11-linked chains target APC/C^{Cdh1} substrates for degradation in vivo. The APC/C-dependent degradation of geminin, Plk1, and securinΔD was triggered in 293T cells in the presence of indicated ubiquitin mutants (WT-ubi, ubi-R11, ubi-R48) by coexpression of Cdh1. The expression levels were analyzed by western blotting.

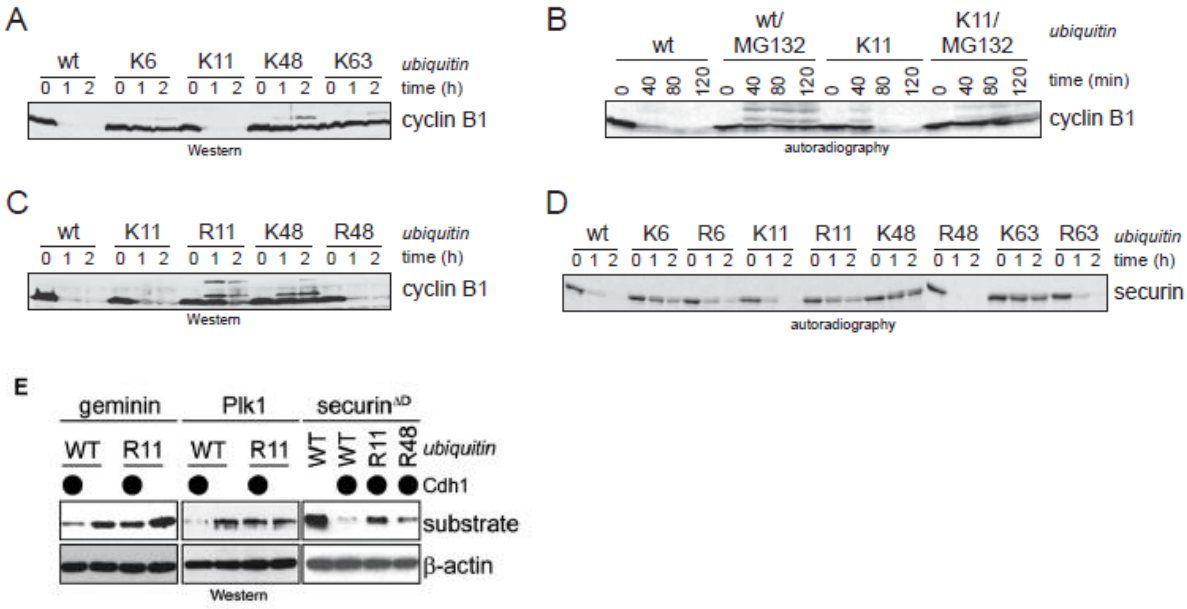
A
wt
K6
K11
K48
K63
ubiquitin
0 1 2 0 1 2 0 1 2 0 1 2 0 1 2
time (h)
cyclin B1
Western
B
wt
wt/ MG132
K11
K11/ MG132
ubiquitin
0 40 80 120 0 40 80 120 0 40 80 120 0 40 80 120
time (min)
cyclin B1
autoradiography
C
wt
K11
R11
K48
R48
ubiquitin
0 1 2 0 1 2 0 1 2 0 1 2 0 1 2
time (h)
cyclin B1
Western
D
wt
K6
R6
K11
R11
K48
R48
K63
R63
ubiquitin
0 1 2 0 1 2 0 1 2 0 1 2 0 1 2 0 1 2 0 1 2 0 1 2 0 1 2
time (h)
securin
autoradiography
E
geminin
Plk1
securinΔD
WT
R11
WT
R11
WT
WT
R11
R48
ubiquitin
Cdh1
substrate
β-actin
Western

Fig. 1-2: APC/C substrates modified with K11-linked ubiquitin chains are recognized by proteasomal receptors for degradation

(A) APC/C^{Cdh1} and UbcH10 assemble chains on cyclin A using ubi-K11 but no other single-lysine mutant in an in-vitro ubiquitination assay. Radiolabeled cyclin A was incubated with purified APC/C^{Cdh1}, UbcH10, E1 and ubiquitin mutants. Ubiquitination of cyclin A was visualized by autoradiography.

(B) APC/C^{Cdh1} and UbcH5c form ubiquitin chains on cyclin A linked through K11, K48, and K63. In-vitro ubiquitination assay of cyclin A was performed as above. UbcH5c was added as an E2 instead of UbcH10.

(C) UbcH5 is less efficient in promoting the degradation of securin Δ D in G1 extracts. G1 extracts were supplemented with ubiquitin mutants and UbcH10 (upper panel) or UbcH5c (lower panel). Degradation of radiolabeled securin Δ D was monitored by autoradiography.

(D) K11-linked chains are recognized by the proteasomal receptor Rad23. The UBA domains of Rad23 were immobilized on beads and incubated with cyclin A that was ubiquitinated in the presence of wt-ubi, ubi-K11, and ubi-R11. Proteins bound by the UBA domains of Rad23 are shown by the letter ‘‘B’’ (bound).

(E) APC/C substrates modified with K11-linked chains are recognized by proteasomal receptors. Cyclin A was ubiquitinated by APC/C^{Cdh1} and UbcH10 in the presence of ubi-K11 and tested for binding to GST (negative control), GST-S5a, and hPlic2. Bound proteins were analyzed by autoradiography.

A

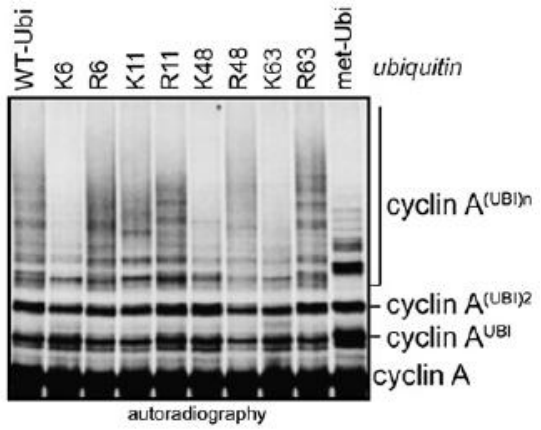
WT-Ubi
K6
R6
K11
R11
K48
R48
K63
R63
met-Ubi
ubiquitin
cyclin A(UBI)n
cyclin A(UBI)2
cyclin AUBI
cyclin A
autoradiography

B

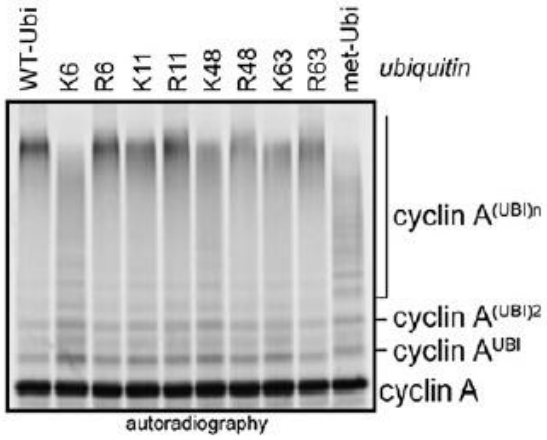
WT-Ubi
K6
R6
K11
R11
K48
R48
K63
R63
met-Ubi
ubiquitin
cyclin A(UBI)n
cyclin A(UBI)2
cyclin AUBI
cyclin A
autoradiography

C

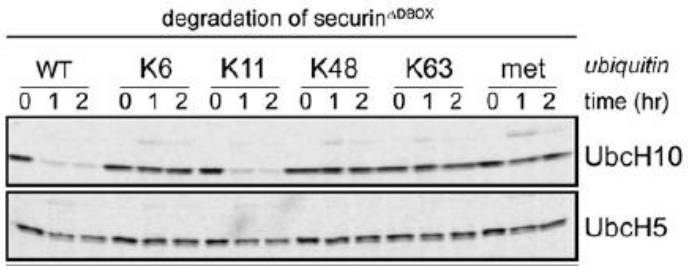
degradation of securinΔDBOX
WT
K6
K11
K48
K63
met
ubiquitin
0 1 2 0 1 2 0 1 2 0 1 2 0 1 2 0 1 2
time (hr)
UbcH10
UbcH5

D

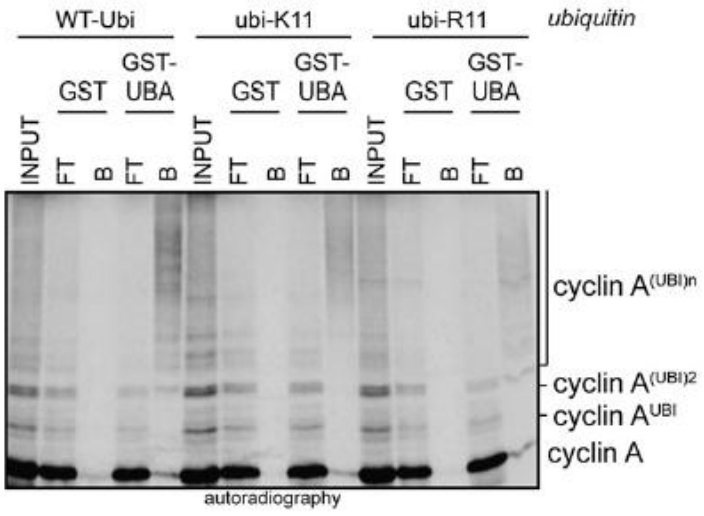
WT-Ubi
ubi-K11
ubi-R11
ubiquitin
GST
GST-UBA
INPUT
FT
B
cyclin A(UBI)n
cyclin A(UBI)2
cyclin AUBI
cyclin A
autoradiography

E

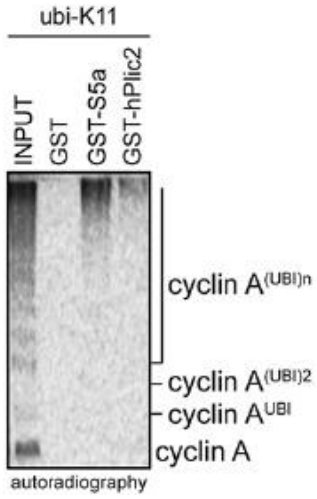
ubi-K11
INPUT
GST
GST-S5a
GST-hPlic2
cyclin A(UBI)n
cyclin A(UBI)2
cyclin AUBI
cyclin A
autoradiography

Fig. 1-3: Identification of a ubiquitin surface important for the assembly of K11-linked ubiquitin chains

(A) Degradation of the APC/C substrate securin in G1 extracts in the presence of ubiquitin mutants, as monitored by autoradiography.

(B) Degradation of the APC/C^{Cdh1} substrate securinΔD in 293T cells is inhibited by overexpression of ubi-R11, ubi-K6A, and ubi-L8A. Cdh1 was coexpressed where indicated (C), and the levels of securinΔD and β -actin were monitored by western blotting.

(C) Ubi-L8A shows defects in promoting ubiquitin chain formation of APC/C substrate in vivo. Securin was coexpressed in 293T cells with 6xHis-ubiquitin mutants. Conjugates were purified on NiNTA-agarose under denaturing conditions and ubiquitinated securin was detected by western blotting. Ubiquitin without lysine residues (‘‘noK’’) is not incorporated into chains, whereas ubi-L8A is less efficient to promote chain formation than ubi-K11.

(D) Localization of mutations that affect APC/C activity in G1 on the surface of ubiquitin. K11 is marked in red; mutants of ubiquitin interfering with APC/C activity are labeled orange; mutants that didn’t affect APC/C activity are marked in green.

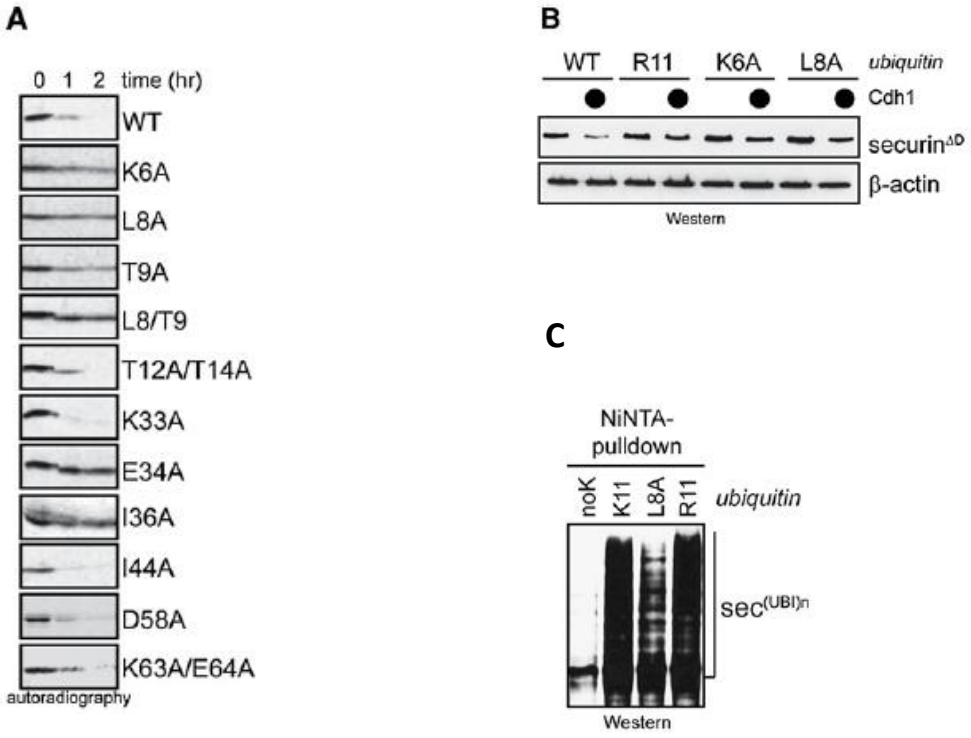
A
0 1 2 time (hr)
WT
K6A
L8A
T9A
L8/T9
T12A/T14A
K33A
E34A
I36A
I44A
D58A
K63A/E64A
autoradiography
B
WT R11 K6A L8A ubiquitin
Cdh1
securin^ΔD
β-actin
Western
C
NiNTA-pulldown
noK K11 L8A R11 ubiquitin
sec^(UBI)n
Western
D
K11 E34 I36
T9
L8
K6
180°

Fig. 1-4: Ubiquitin Deficient of K11 Causes Cell Cycle Arrest During Early Embryogenesis *of Xenopus tropicalis*

(A) K11 linkages are required for rapid cell-cycle progression in embryos of Xenopus tropicalis. One cell of X. tropicalis embryos at the two-cell stage was injected with recombinant WT-ubi or ubi-R11 and a fluorescent tracer. Injected cells were followed by fluorescence microscopy, and cell division was monitored by phase microscopy.

(B) K11 linkages are required for X. tropicalis development. Injected embryos were allowed to develop to the tadpole stage. The percentage of embryos without developmental aberrations (‘‘normal’’) and that of viable embryos was determined. Error bars represent standard error from three independent experiments.

A

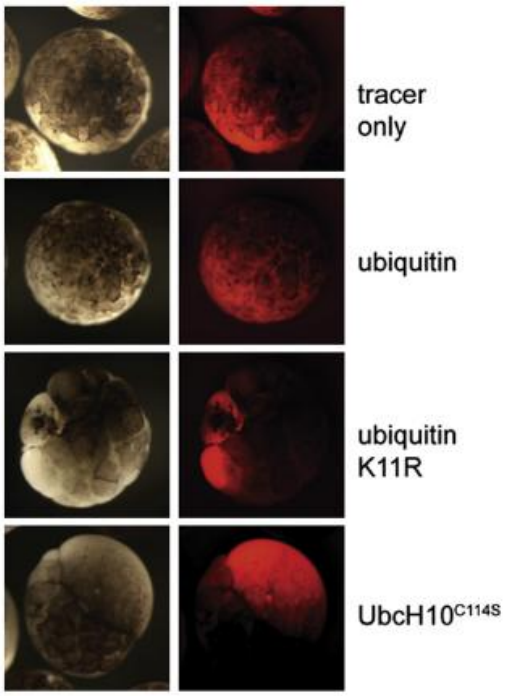
tracer
only
ubiquitin
ubiquitin
K11R
UbcH10C114S

B

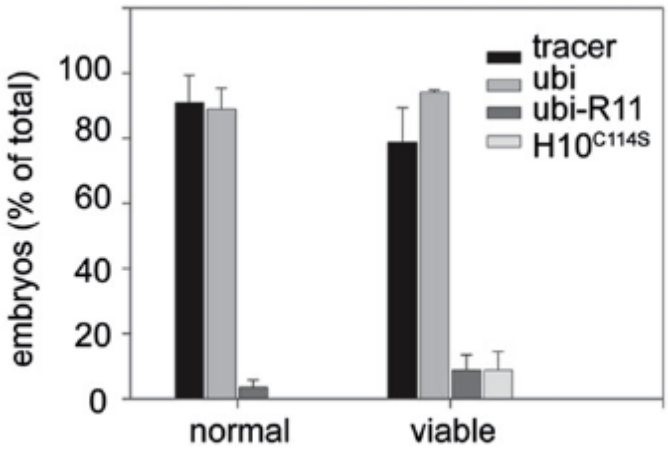
embryos (% of total)
100
80
60
40
20
0
normal
viable
tracer
ubi
ubi-R11
H10C114S

Chapter Two

Identification of Cullin-3 as an Important E3 in Mouse Embryonic Stem Cells

2.1 Introduction

Embryonic stem cells are derived from the inner cell mass of the blastocyst. They have the capacity to replicate themselves and to differentiate into various cell types, which makes them a valuable resource in research and regenerative medicine. Although numerous publications have reported the identification of genes required for pluripotency, lineage-specific differentiation, or reprogramming, little is known about how embryonic stem cells exit from a rapidly cycling pluripotent state to a slowly dividing differentiated state. Ubiquitination regulates the cell cycle by controlling the stability of key regulators, such as cyclins or checkpoint proteins. Although a lot is known about the ubiquitin-mediated cell cycle control in somatic cells, enzymes and substrates of the ubiquitin-dependent control of stem cell proliferation and differentiation remain poorly characterized. Compared with somatic cells, embryonic stem cells have a much more rapid cell cycle, primarily due to the shortened G1 state. Interestingly, the regulation of APC/C, which controls the stability of many G1 cyclins, is different in ES cells than in somatic cells. For example, the protein levels of UbcH10 and E2S, the two APC/C specific E2s being degraded during G1 stage of somatic cells, remain constant during the cell cycle of ES cells (data not shown). In addition to cell cycle regulation, ubiquitination and proteasomal system has been reported to be an essential regulator in other stem cell systems. APC/C^{Cdh1} is involved in neural development by degrading Id2, a transcriptional inhibitor in differentiation (Lasorella, et. al., 2006). REST, another repressor of neurogenesis, is ubiquitinated by SCF^{bTrcp} during differentiation (Westbrook, et. al., 2008). The E3 ligase SCF^{Fbw7} regulates the transition of hematopoietic stem cells from quiescent state to differentiation state by controlling the stability of its substrate c-myc (Reavie, et. al., 2010). In addition, mutations in SCF^{Fbw7} and its substrate Notch account for ~75% of T-cell acute lymphoblastic leukemia (T-ALL) (Thompson, et. al., 2007).

Despite the fact that ubiquitin/proteasome system (UPS) has been shown to be critical for the proliferation and differentiation of embryonic stem cells (Szutorisz, et. al., 2006), very few ubiquitin enzymes and their substrates have been isolated as the key regulator. To address this question, I have developed an siRNA-based screening strategy to isolate ubiquitination enzymes required for mouse embryonic stem cell proliferation and differentiation. This approach allowed me to identify the ubiquitin ligase Cullin-3 (Cul3) as an essential regulator of cell division in embryonic stem cells. Interestingly, depletion of Cul3 has little effect on the expression of pluripotent genes or major cell cycle regulators. A detailed, siRNA- and microscopy based analysis showed that Cul3 controls mES cell division by participating in an integrin-Src-Rac-actin dependent signaling pathway that regulates the adhesion of stem cells to the extracellular matrix (ECM). In this Chapter, I will introduce the identification and characterization of Cul3 as an important regulator in the integrin pathway of mouse ES cells.

2.2 Results

2.2.1 Cullin-3 (Cul3) is an Essential E3 for the Proliferation and Morphology of Mouse Embryonic Stem Cells

To isolate ubiquitin ligases essential for embryonic stem cells, I developed an siRNA screen in D3 mouse ES cells (as shown in Fig. 2-1A). The initial screen included about 40 ligases and at least two different siRNA oligos were designed for each gene. Three days post transfection, pictures were taken using bright-field microscopy. Out of the 40 ligases I have screened, the depletion of Cullin-3 (Cul3) leads to a dramatic change in ES cell morphology and obvious compromised cell growth, which is not seen when other members of the Cullin family are depleted (Fig. 2-1B). To confirm the specificity of the Cul3 phenotype, five siRNA oligos targeting distinct regions of Cul3 mRNA were tested in mouse ES cells. Three of the five oligos reproduced the phenotype as seen in the screen, whereas the other two had a moderate phenotype. Notably, the strength of the phenotype tightly correlates with the knockdown efficiency of the different oligos (Fig. 2-1C), which confirms the phenotype of compact colonies to be attributed to Cul3 knockdown but not other non-specific effect.

In addition to the morphological changes, depletion of Cul3 also significantly inhibits the proliferation of ES cells (Fig. 2-2A). Using FACS analysis, I saw a slight increase in G2/M fraction of cells when Cul3 is depleted (Fig. 2-2B). This could be due to the deficiency in mitotic progression and cytokinesis upon Cul3 knockdown as previously reported (Sumara, et. al., 2007). Indeed, when plated at a low density, I can observe about 2-3% of Cul3-depleted ES cells to be multinucleated (Fig. 2-2C). Considering the low percentage of multi-nucleated cells, it is unlikely that mitotic defect is the only reason for the reduced growth rate of Cul3-depleted cells, which I will discuss later.

2.2.2 Depletion of Cul3 Does Not Affect the Pluripotency of ES Cells

Undifferentiated ES cells express high levels of transcriptional factors called Oct4, Sox2 and Nanog, which control the expression of a number of downstream genes that promote pluripotency and cell proliferation. When being grown under differentiating conditions, e.g. upon removal of LIF and in suspension culture, the expression of these pluripotent markers quickly go down and the tissue-specific genes are highly up-regulated. The ES cells also undergo morphological changes and grow into ball-like cell aggregates called embryoid bodies. Cultured for a longer time under defined conditions, these embryoid bodies can differentiate into various cell lineage. On the other hand, it has been reported by many labs that expression of exogenous Oct4, Sox2 and Nanog in differentiated cells like fibroblasts is sufficient to reverse the differentiation process and convert the fibroblast to ES cell-like pluripotent cells, called induced pluripotent stem cells (iPSC). This further highlights the importance of these transcriptional factors in maintaining ES cell pluripotency.

The cell compaction phenotype upon Cul3 depletion resembles embryoid body, the early stage of ES cell differentiation. To test whether Cul3 depletion has any effect on ES cell pluripotency and differentiation, I performed Cul3 knockdown in mouse ES cells and stained for Oct4 expression, the hallmark of pluripotency (Fig. 2-3A). Interestingly, Cul3-depleted cells express the same level of Oct4 compared with control cells although they are morphologically distinct. Undifferentiated ES cells also display high level of alkaline phosphatase activity, which is often used as a marker for pluripotency. Thus, ES cells treated with scramble siRNA, siCul3 or siOct4 as control were plated at low density to allow formation of single colonies. The

pluripotency of each colony was determined by its morphology and alkaline phosphatase activity as shown in red. Although the total number of colonies of Cul3-depletion was significantly lower than control, which is due to the decrease in cell proliferation, the percentage of AP-positive undifferentiated colonies was unaffected (Fig. 2-3B). This again points to the fact that Cul3-depletion does not affect the pluripotency of ES cells.

Next, I tested whether the expression of any lineage-specific genes was altered upon Cul3 depletion. Not surprisingly, Cul3-depleted ES cells didn't show significantly elevated expression of cell type-specific markers as determined by RT-qPCR (Fig. 2-3C). Previous study implicated Cul3 in regulation of Wnt signaling pathway by ubiquitinating its regulator Dishevelled (Dvl2) (Angers, et. al., 2006). However, our expression analysis didn't show any remarkable change in the expression of downstream genes of Wnt signaling pathway upon Cul3 depletion (Fig. 2-3D). In fact, the microarray data demonstrate that Cul3 is probably the only gene whose expression is significantly altered (Fig. 2-3E), indicating that Cul3 is not directly involved in the transcriptional network of ES cells.

2.2.3 Cul3 is Involved in Integrin-Src-Rac-Actin Pathway

As shown above, Cul3 depletion does not affect the pluripotency or differentiation of mouse ES cells. Then we reasoned that the dramatic morphological changes could be attributed to changes in cytoskeletal organization, or intracellular or cell-matrix interaction. To test this hypothesis, I set up another siRNA screen in D3 mouse ES cells against genes involved in cytoskeleton arrangement and cell adhesion. Interestingly, depletion of a number of genes involved in Integrin-Src-Rac-Actin pathway fully mimicks Cul3 depletion in mouse ES cells, with the cell compaction phenotype. These genes include the Src substrate CAS, and Rac1 and Iqgap1, which are CAS substrates and regulators of F-actin assembly. In contrast, depletion of Cdc42, another actin regulator, or E-cadherin, another adhesion molecule, produced distinct phenotypes (Fig. 2-4A). Upon binding to extracellular matrix (ECM), the heterodimeric integrin complex undergoes oligomerization and autophosphorylation on its cytosolic tyrosine residue, and thereby recruits the Src kinase. The activated Src kinase then phosphorylates and activates the CAS, which forms a complex with Dock180 and functions as a Rac1 GEF. The activated Rac1 regulates the formation of lamellipodia and promotes cell spreading (Fig. 2-4B). In addition, Rac1 antagonizes with RhoA, which promotes the formation of stress fibers and leads to cell contraction.

To confirm that Cul3 is a bona-fide regulator of Integrin-Src-Rac-Actin pathway, we designed a synthetic lethality assay using dasatinib, a Src kinase inhibitor. Dasatinib treatment by itself does not produce a strong phenotype in ES cells even at a high concentration. However, when used together with diluted siCul3 oligo which does not have an effect by itself either, dasatinib with increasing concentration causes cell compaction in ES cells (Fig. 2-4D). Depletion of RhoA, an antagonist of Rac1 activity, or treatment with RhoA inhibitor Y27632, both rescue the Cul3-depletion phenotype (Fig. 2-4C). Most interestingly, depletion of Cul3 causes dramatic diminishment of integrin localization on the surface of ES cell colonies (Fig. 2-4E). These all point to the fact that Cul3 regulates the cell adhesion to ECM and cytoskeletal organization by affecting the integrin localization. Notably, the activation of Integrin-Src

pathway also promotes cell proliferation by activating MAPK pathway, which is consistant with the growth defect upon Cul3 depletion as discussed above. The Cul3-regulated integrin pathway is especially important in ES cells as depletion of Cul3 in 3T3 mouse fibroblasts does not lead to significant morphological changes (Fig. 2-4F. The knockdown efficiency of Cul3 was comparable in both cell lines – data not shown).

2.3 Discussion

Cul3 knockout mouse is embryonic lethal at a very early stage (E6.5, Singer, et. al., 1999), however, the molecular mechanism behind it is largely unknown. Here, using mouse embryonic stem cell as a model system, I identified Cul3 as an essential regulator for ES cell proliferation and morphology by participating in the Integrin-Src-Rac-Actin signaling pathway. By interacting with the extracellular matrix (ECM), integrin activates a cascade of cellular events which promote cell proliferation and cytoskeleton rearrangement. Our data indicates that Cul3 positively regulates the integrin pathway by facilitating integrin localization on plasma membrane, a very upstream step in the integrin signaling pathway. However, this could happen at several possibilities: Cul3 may function in the deposition of ECM, or it can modulate the recognition of integrin with ECM, or it may facilitate the intracellular trafficking and recycling of integrin. To distinguish these possibilities and fully dissect the function of Cul3, it is essential to isolate the substrate(s) of Cul3 in ES cells, which I will discuss later in the follow-up chapters.

2.4 Material and Methods

Antibodies

Antibodies used in this study are listed as follows: Oct3/4 (Santa Cruz, sc-8628), Vinculin (Sigma, V9131-.2ml), β1-integrin (BD Transduction Laboratories, 610467), Alexa 488 Phalloidin (Invitrogen, A12379), Rhodamine Phalloidin (Invitrogen, R415)

Cell Culture

The D3 mouse embryonic stem cells (mESC) were maintained in ESC medium containing 15% FBS, 1x sodium pyruvate, 1x NEAA, 1mM β-ME and 1000u/ml LIF (Millipore, cat. # ESG1107) in GIBCO Dulbecco's Modified Eagle Medium, and grown on 0.1% gelatin-coated tissue culture plates. NIH3T3 cells were maintained in DMEM plus 10% FBS.

SiRNA Screen in Mouse ES Cells

siRNA oligos against 40 mouse ubiquitin E3 enzymes were pre-designed by Qiagen and handled as instructed. Two different siRNA oligos against each gene were included in the initial screen. To perform siRNA screen in a 96-well plate, 10pmol of siRNA oligos and 0.25ul of Lipofectamine2000 were pre-incubated in 20ul of OPTIMEM for each well for 15min at room temperature. The D3 mouse embryonic stem cells were trypsinized and seeded at 15000 cells/well in 80ul of ESC medium on top of the siRNA mixture in 0.1% gelatin-coated 96-well plate. Fresh media was added to the cells the next day and the morphology of ES cell colonies were examined under the bright-field microscope at 48 or 72 hours post transfection. To validate Cul3 as a hit, we ordered two more siRNA oligos from Qiagen and one from Dharmacon

targeting different sites of the sequence. The severity of the phenotype corresponds closely with the knockdown efficiency of different oligos as confirmed by both western blot and qRT-PCR analysis.

Drug Treatment of Mouse ES Cells

To study the synthetic lethal effect of Src-inhibition with Cul3 knockdown, wildtype and Cul3-depleted D3 mouse ES cells were treated with an increasing concentration of Dasatinib at 0, 25, 50, 100nM for 18 hours before the phenotypes were analyzed by light microscopy. To study the effect of Rho-inhibition with Cul3 knockdown, the Cul3-depleted D3 mouse ES cells were treated with ROCK inhibitor Y27632 at 10uM for 24 hours before phenotype analysis.

Cell cycle analysis

To compare the growth rate of wildtype, Cul3-depleted and H10/E2S-depleted mouse ES cells, the cells were treated with scramble siRNA, Cul3 siRNA, or UbcH10/E2S siRNA and seeded at $3x10^5$ cells/well in gelatin-coated 6-well plates. The cells were trypsinized at 2, 3 and 4 days post transfection and counted by hemocytometer.

To analyze the cell cycle profile of mouse ES cells upon Cul3 depletion, the cells were treated with control or siRNA against Cul3 and seeded at $3x10^5$ cells/well in a gelatin-coated 6-well plate. 48 hours after transfection, cells were collected by trypsinization and fixed in -20C 70% ethanol for at least 1 hour. After washing with PBS/2%FBS, cells were resuspended in 300ul propidium iodide solution (69uM propidium iodide in 38mM NaCitrate pH7.4) with 0.67mg/ml RNaseA, and incubated at 37C in dark for 30min. After brief washing, cells were resuspended in 800ul of PBS at about 2×10^6 cells/ml, transferred to FACS tubes and applied to Beckman-Coulter EPICS XL Flow Cytometer for analysis.

Quantitative real-time PCR analysis

I used TRIzol (Invitrogen, cat. # 15596-026) and chloroform to extract total RNA from cells. The first-strand cDNAs were synthesized by using Revertaid first strand cDNA synthesis kit (Fermentas, cat. # K1621). Gene-specific primers for RT PCR were designed by using NCBI Primer-Blast. The quantitative real-time PCR reaction was done with Maxima SYBR Green/Rox qPCR system (Fermentas, cat. # K0221).

Immunofluorescence Staining & Confocal microscopy

Cells were fixed in 4% paraformaldehyde and permeablized with 0.5% TritonX-100 in block buffer (1X TBS buffer with 2% BSA). Cells were then incubated with primary antibodies against specific proteins, such as Viculin for 2 hours and secondary antibodies (Invitrogen, Alexa Fluor® 546 goat anti-rabbit IgG (H+L), cat. # A-11035 ; Alexa Fluor 488 goat anti-mouse IgG (H+L), cat. # A11001) together with HOECHST 33342 (VWR, 100057-320) for 1 hour at room temperature followed by extensive washing. Pictures were taken by using Zeiss LSM 510 and 710 Confocal Microscope systems and analyzed with LSM image browser and Imaris 3D imaging processing software.

Microarray

To compare gene expression profiles of wildtype vs Cul3-depleted mouse ES cells, D3 mouse ES cells were transfected with control or Cul3 siRNA and grown on gelatin-coated 6-well plate. 48 hours later, total RNA was extracted by TRIzol and chloroform, and further purified using

RNeasy Mini Kit (Qiagen, cat. # 74104). Microarray assay was performed by the Functional Genomics Laboratory at UC Berkeley using an Affymetrix Mouse 430A 2.0 chip.

Table S1. List of siRNA oligos

oligo name	Targeted sequence (5' – 3')
mCul3 #1	GAAGGAATGTTTAGGGATA
mCul3 #2	GGAAGAAGATGCAGCACAA
mCul3 #3	GGTGATGATTAGAGACATA
mCul3 #4	CAACTTTCTTCAAACACTA
mCul3 #5	CATTATTTATTGATGATAA
mOct4	AGGCAAGGGAGGTAGACAA
mCdc42 (pool of 4 oligos)	GATCTAATTTGAAATATTA
	GGATTGAGTTCCTAATTAA
	AGAGGATTATGACAGACTA
	AAATCAAACTAAAGATTAA
mBcar1/CAS (pool of 4 oligos)	GACTAATAGTCTACATTTA
	GGAGGTGTCTCGTCCAATA
	CTATGACAATGTTGCTGAA
	GGGCGTCCATGCTCCGGTA
mSrc (pool of 4 oligos)	CCCTTGTGTCCATATTTAA
	CCACGAGGGTTGCCATCAA
	CAGACTTGTTGTACATATT
	GCAACAAGAGCAAGCCCAA
mRhoG (pool of 4 oligos)	GGTTTACCTAAGAGGCCAA
	GCTGTGCCTTAAGGACTAA
	GCACAATGCAGAGCATCAA
	GGCGCACCGTGAACCTAAA
mRhoA (pool of 4 oligos)	GGATTTCCTAATACTGATA
	GAAAGTGTATTTGGAAATA
	AGCCCTATATATCATTCTA
	CGTCTGCCATGATTGGTTA
mRac1 (pool of 4 oligos)	GGTTAATTTCTGTCAAACA
	GCGTTGAGTCCATATTTAA
	GCTTGATCTTAGGGATGAT
	GGAGTAATTCAACTGAATA
mCdh1/E-cadherin (pool of 4 oligos)	GGAGGAGAACGGTGGTCAA
	CGCGGATAACCAGAACAAA
	CCATGTTTGCTGTATTCTA
	GGGACAATGTGTATTACTA
mIqgap1 (pool of 4 oligos)	ACATGATGATGATAAACAA
	GGTTGATTTCACAGAAGAA
	GTATAAATTTATTTCTTAA
	GGTGGATCAGATTCAAGAA
mCul1 (pool of 2 oligos)	GCATGATCTCCAAGTTAAA
	CGTGTAATCTGCTATGAAA

mCul2 (pool of 2 oligos)	GCGCTGATTTGAACAATAA
	CCAGAGTATTTATATCTAA
mCul4a (pool of 2 oligos)	GTGTGATTACCATAATAAA
	CCAGGAAGCTGGTCATCAA
mCul5 (pool of 2 oligos)	CCCTCATATTTACAGCAAA
	ACATGAAGTTTATAATGAA
mCul7 (pool of 2 oligos)	GCATCAAGTCCGTTAATAA
	GGATGTGATTGATATTGAA

Fig. 2-1: siRNA screen identifies Cullin-3 as an essential E3 ligase in D3 mouse ES cells

(A) Schematic flowchart of siRNA screen in D3 mouse ES cells.

(B) Depletion of Cul3 but not other members of the Cullin family leads to a dramatic morphological change as well as compromised cell growth in mouse ES cells. The left panel shows the depletion of each of the Cullin family. The right panel shows the knockdown efficiency of each Cullin using RT-qPCR.

(C) The severity of the Cul3 phenotype in mouse ES cells closely correlates with the knockdown efficiency of different siRNA oligos. Left top: the knockdown efficiency of different siRNA oligos is determined by western blotting and RT-qPCR respectively. 'NC' represents negative control siRNA. Left bottom: ES colonies with compact morphology are counted for each of the five oligos. A total of about 30 colonies are present in one well of the 96-well format. Right: bright-field pictures of mouse ES cells depleted with Cul3 using each of the five oligos.

A

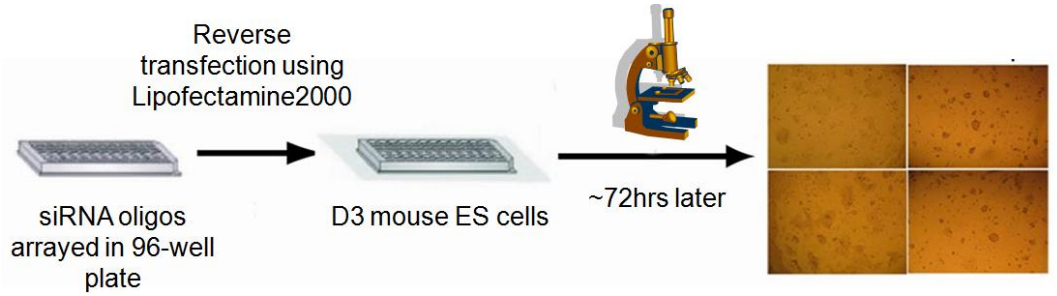
Reverse
transfection using
Lipofectamine2000
siRNA oligos
arrayed in 96-well
plate
D3 mouse ES cells
~72hrs later

B

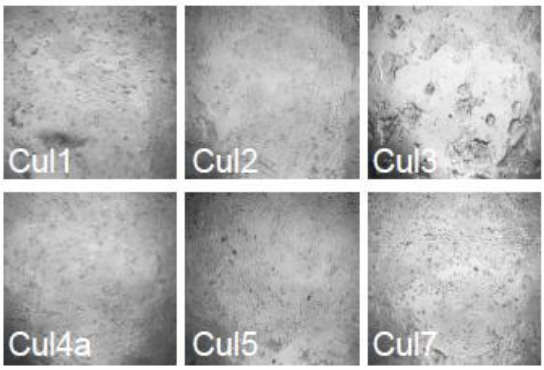
Cul1
Cul2
Cul3
Cul4a
Cul5
Cul7

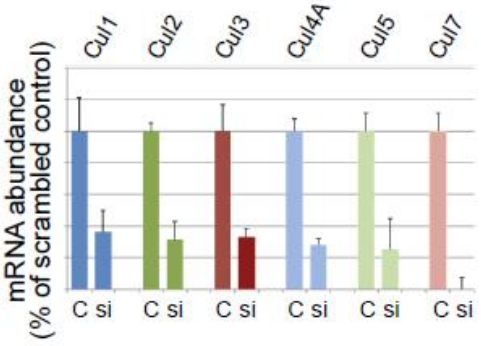
mRNA abundance
(% of scrambled control)
Cul1
Cul2
Cul3
Cul4A
Cul5
Cul7
C si

C

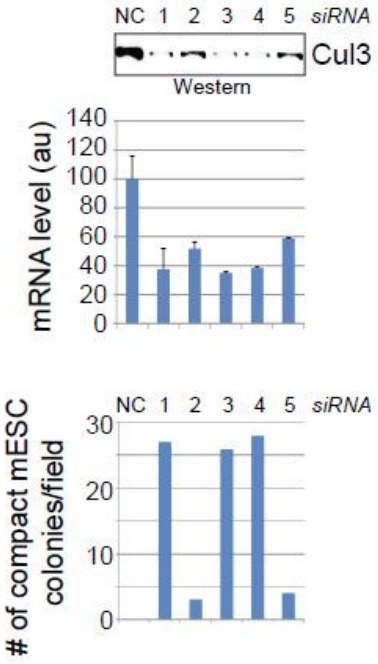
NC 1 2 3 4 5 siRNA
Cul3
Western
mRNA level (au)
140
120
100
80
60
40
20
0
NC 1 2 3 4 5 siRNA
# of compact mESC
colonies/field
30
20
10
0

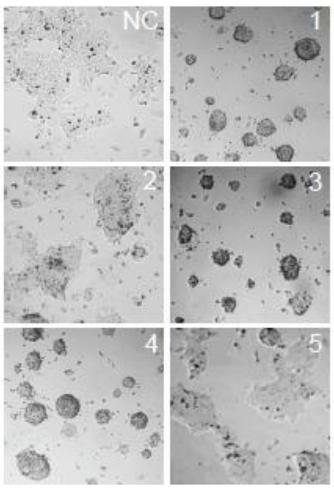
NC
1
2
3
4
5

Fig. 2-2: Depletion of Cul3 affects the proliferation of ES cells

(A) Depletion of Cul3 decreases the growth rate of mouse ES cells. Left panel: D3 mouse ES cells were treated with control siRNA, siCul3-1 or siCul3-4 respectively and cultured on gelatin-coated dish. Cell numbers were counted at indicated time points post transfection. Right panel: the growth rate of Cul3-depleted cells was compared with cells depleted with UBE2S and UbcH10, which are known mitotic regulators.

(B) FACS analysis of mouse ES cells treated with either control siRNA (left) or siCul3 (right). Cul3-depleted cells show a slight increase (~6%) in G2/M population.

(C) A small percentage of ES cells are multi-nucleated upon Cul3 knockdown. Mouse ES cells were transfected with control siRNA, siCul3-1 or siCul3-2 and seeded at low density. Two days post transfection, cells were fixed and stained with DAPI and phalloidin 488 to visualize the nucleus and actin filaments respectively.

A

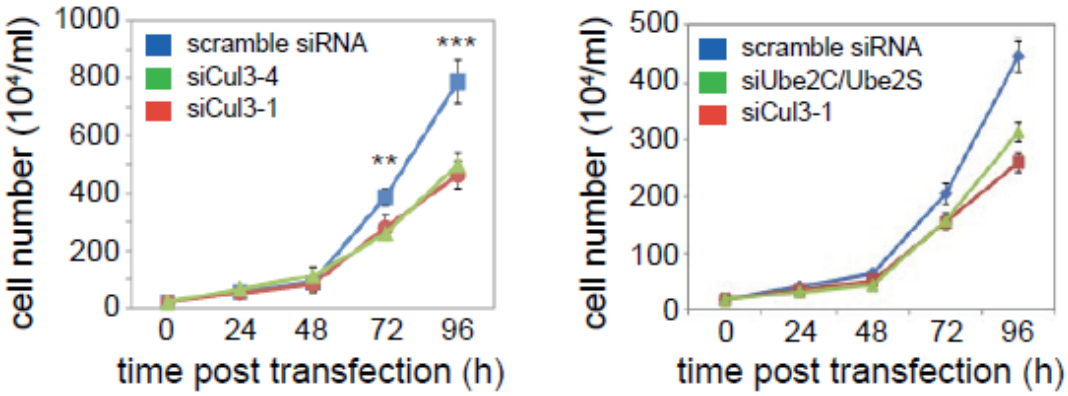
cell number (10⁴/ml)
1000
800
600
400
200
0
scramble siRNA
siCul3-4
siCul3-1
***
**
0
24
48
72
96
time post transfection (h)
cell number (10⁴/ml)
500
400
300
200
100
0
scramble siRNA
siUbe2C/Ube2S
siCul3-1
0
24
48
72
96
time post transfection (h)

B

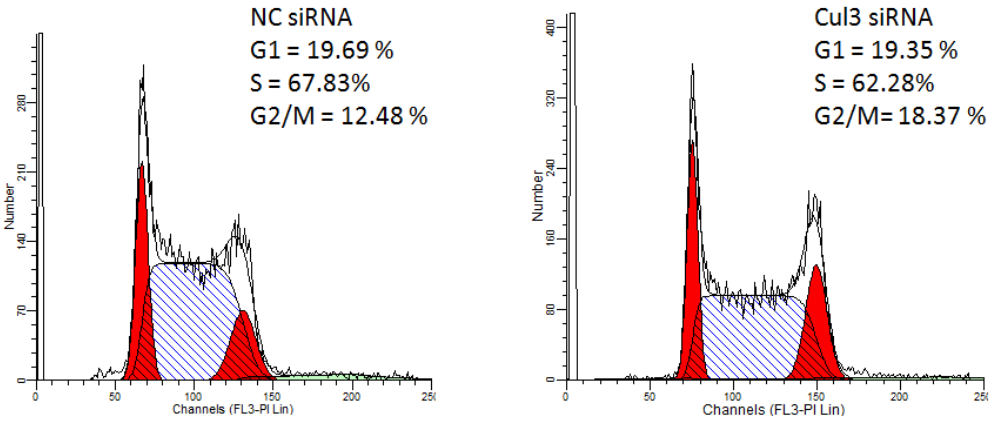
NC siRNA
G1 = 19.69 %
S = 67.83%
G2/M = 12.48 %
Number
Channels (FL3-PI Lin)
Cul3 siRNA
G1 = 19.35 %
S = 62.28%
G2/M= 18.37 %
Number
Channels (FL3-PI Lin)

C

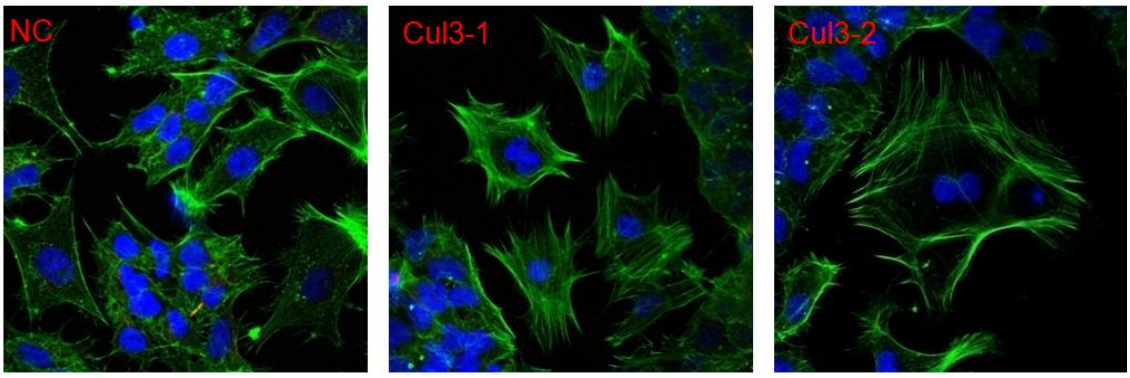
NC
Cul3-1
Cul3-2

Fig. 2-3: Depletion of Cul3 does not affect the pluripotency or differentiation of ES cells

(A) Depletion of Cul3 does not affect the expression of Oct4, a transcriptional factor essential for pluripotency. Mouse ES cells were treated with control siRNA, siCul3 or siOct4, and stained for Oct4 expression by immunofluorescence staining.

(B) Depletion of Cul3 does not affect the pluripotency of mouse ES cells as shown by alkaline phosphatase(AP) assay. Left panel: mouse ES cells treated with insicated siRNA were seeded at low density to allow formation of single colonies. Five days later, the plates with colonies were stained for alkaline phosphatase activity. Right panel: quantification of the numbers of undifferentiated, partially differentiated and differentiated colonies on each plate.

(C) Lineage-specific gene expression is not significantly induced by Cul3 knockdown. Mouse ES cells transfected with scramble, siCul3 or siOct4 were subject to RT-qPCR analysis for expression of genes of all three germ layers.

(D) Cul3 depletion does not significantly affect gene expression in Wnt signaling pathway. Mouse ES cells transfected with either scramble siRNA or siCul3 were analyzed for the expression of target genes in Wnt signaling pathway by RT-qPCR.

(E) Cul3 depletion does not affect the global gene expression in mouse ES cells. Wildtype or Cul3-depleted ES cells were subject to whole genome mRNA microarray analysis. The relative mRNA levels of each gene were plotted and the spots representing Cul3 mRNA were circled in red.

A

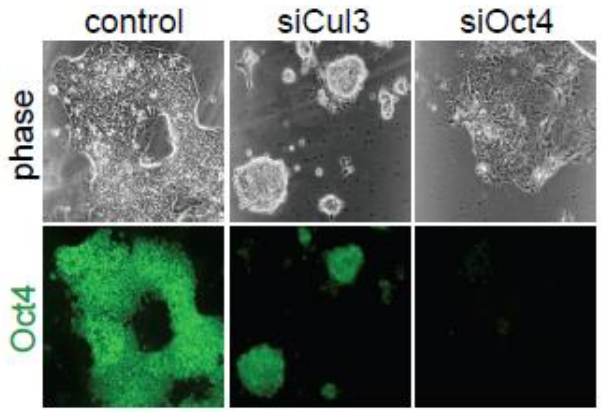
control
siCul3
siOct4
phase
Oct4

B

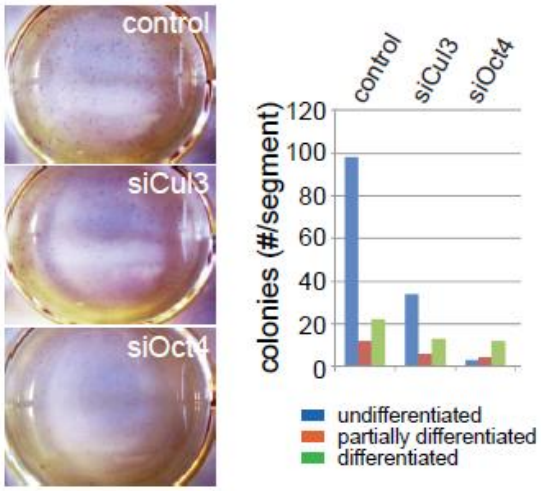
control
siCul3
siOct4
colonies (#/segment)
120
100
80
60
40
20
0
undifferentiated
partially differentiated
differentiated

C

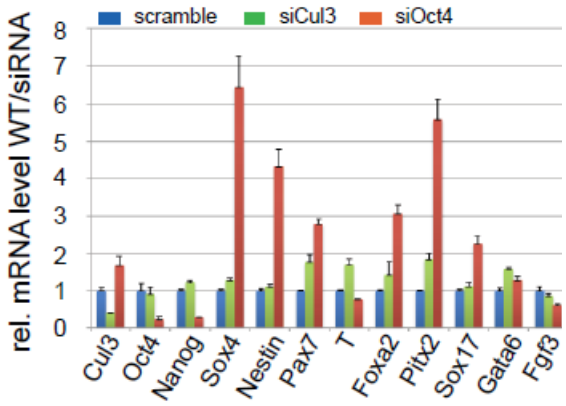
scramble
siCul3
siOct4
rel. mRNA level WT/siRNA
8
7
6
5
4
3
2
1
0
Cul3
Oct4
Nanog
Sox4
Nestin
Pax7
T
Foxa2
Pitx2
Sox17
Gata6
Fgf3

D

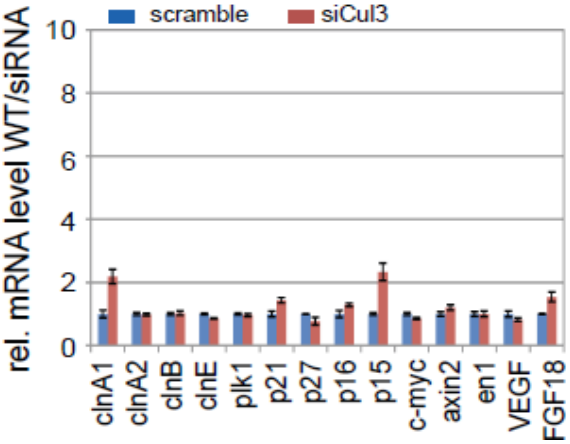
scramble
siCul3
rel. mRNA level WT/siRNA
10
8
6
4
2
0
clnA1
clnA2
clnB
clnE
plk1
p21
p27
p16
p15
c-myc
axin2
en1
VEGF
FGF18

E

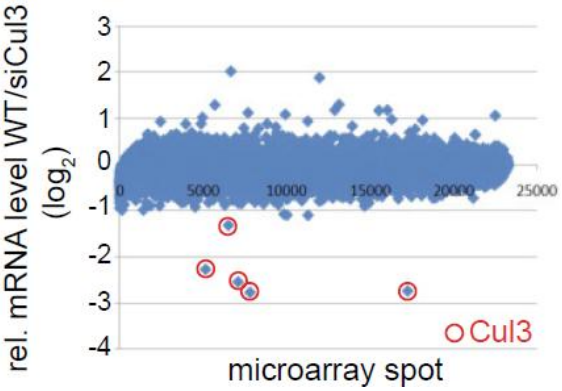
rel. mRNA level WT/siCul3 (log2)
3
2
1
0
-1
-2
-3
-4
0
5000
10000
15000
20000
25000
Cul3
microarray spot

Fig. 2-4: Cul3 is a positive regulator in Integrin-Src-Rac-Actin pathway

(A) Suppression of the Integrin-Src-Rac-Actin pathway by RNAi mimicks the Cul3-depletion phenotype. An siRNA screen in mouse ES cells against genes involved in cytoskeletal arrangement and cell adhesion was performed as previously described. Cells were fixed and subject to immunofluorescence staining against F-actin (phalloidin red) and vinculin (green).

(B) Binding to ECM activates the Integrin-Src-Rac-Actin pathway and alters the morphology of cells.

(C) Inhibition of RhoA activity rescues the Cul3-depletion phenotype. Mouse ES cells depleted with Cul3 were either co-transfected with siRhoA or treated with RhoA inhibitor. Cells were fixed and stained against F-actin (red) and vinculin (green).

(D) Synthetic lethality of Src inhibitor dasatinib with Cul3 depletion in ES cells. Cells were treated with increasing concentration of dasatinib in the presence or absence of diluted siCul3. Pictures were taken under light microscopy.

(E) Cul3-depletion causes mislocalization of integrin in ES cells. Cells were transfected with either scramble siRNA or siCul3 and stained for F-actin (red) and β 1-integrin (green).

(F) Cul3-mediated integrin pathway is especially important in ES cells. Both mouse ES cells and mouse fibroblasts were transfected with siCul3 and the morphology of each cell line was visualized using bright-field and confocal microscope.

A

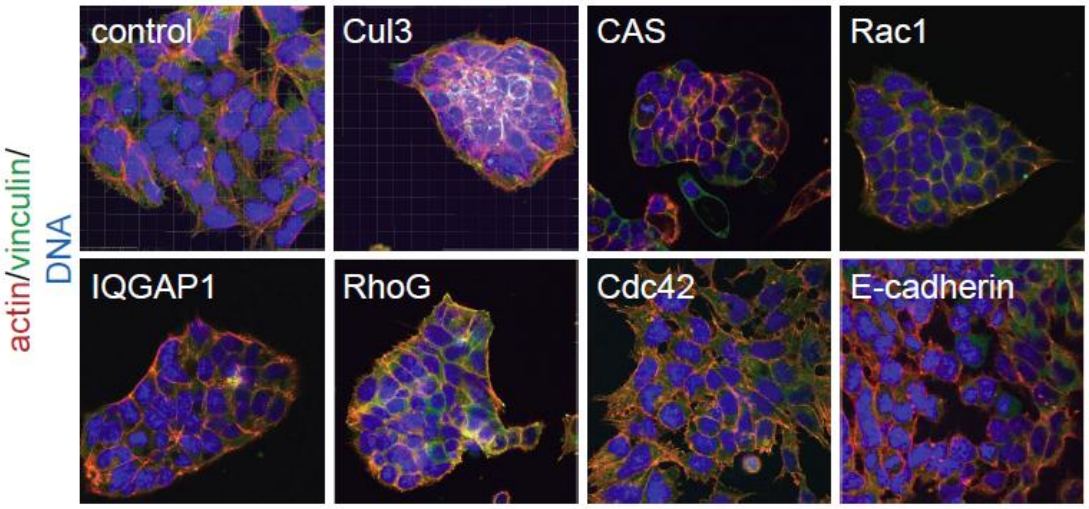
actin/vinculin/
DNA
control
Cul3
CAS
Rac1
IQGAP1
RhoG
Cdc42
E-cadherin

B

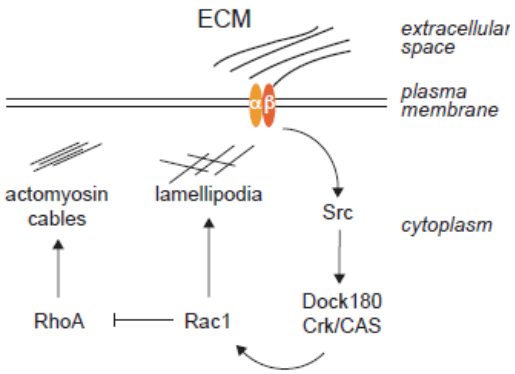
ECM
extracellular space
plasma membrane
actomyosin cables
lamellipodia
Src
cytoplasm
RhoA
Rac1
Dock180
Crk/CAS

C

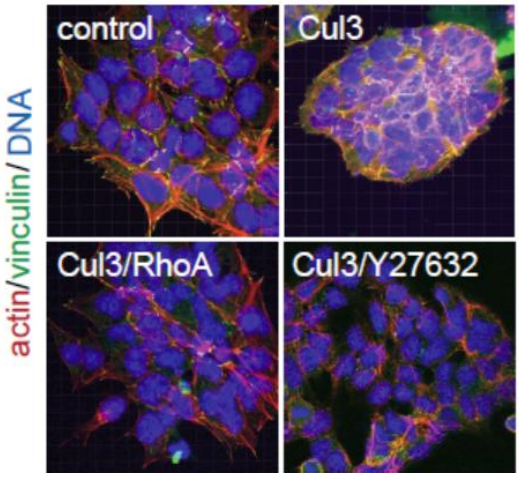
actin/vinculin/ DNA
control
Cul3
Cul3/RhoA
Cul3/Y27632

D

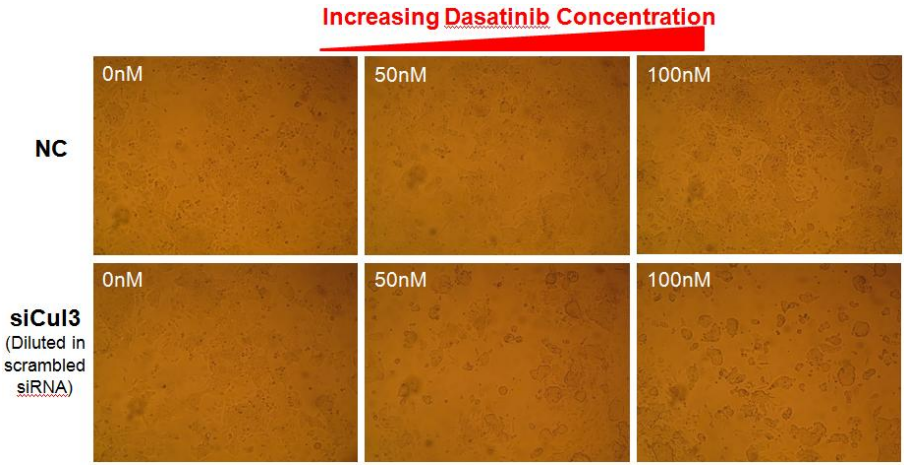
Increasing Dasatinib Concentration
NC
siCul3
(Diluted in scrambled siRNA)
0nM
50nM
100nM
0nM
50nM
100nM

E

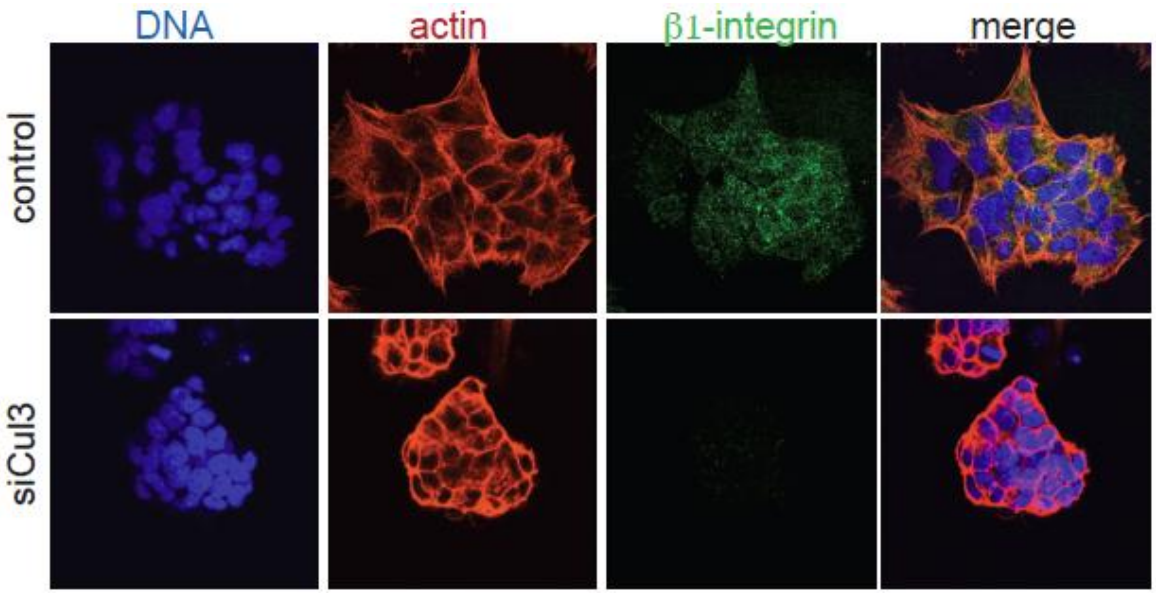
DNA
actin
β1-integrin
merge
control
siCul3

F

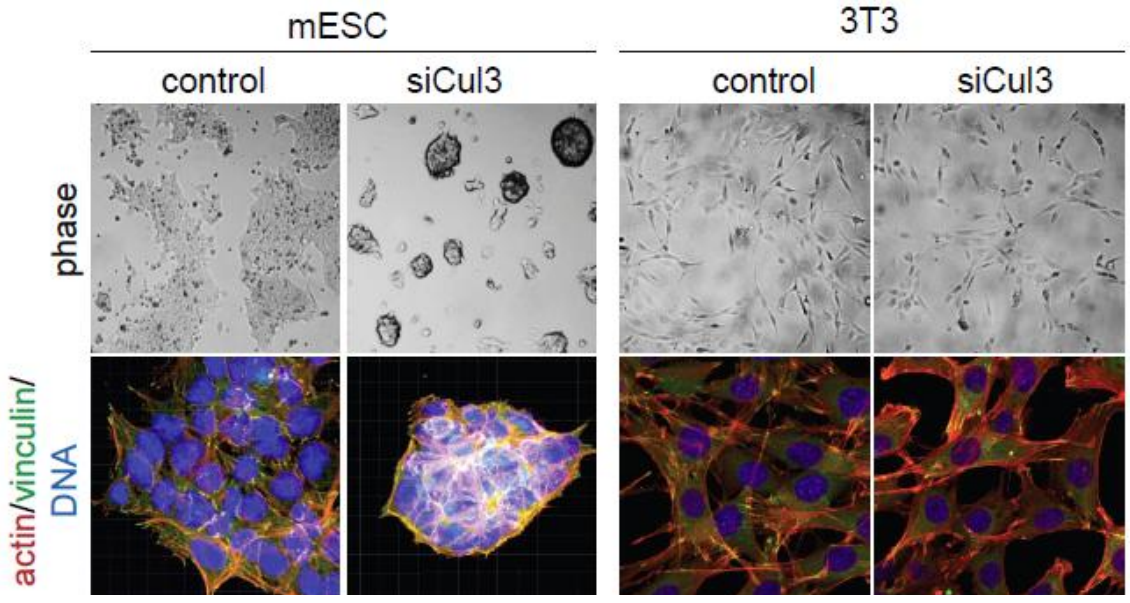
mESC
3T3
control
siCul3
control
siCul3
phase
actin/vinculin/
DNA

Chapter Three

Identification of Klhl12 as ESC-Specific Substrate Adaptor for Cul3

3.1 Introduction

The Cullin3-based ubiquitin ligases belong to a superfamily of multi-subunit RING-class E3 ligases called cullin-RING ubiquitin ligases (CRLs) with a cullin scaffold protein and a catalytic RING subunit, Rbx1 or Rbx2. There are six closely related cullins in human genome, Cul1, Cul2, Cul3, Cul4A, Cul4B, Cul5 (Zimmerman, et. al., 2010). Another three genes Cul7, PARC and APC2 exhibit some homology to Cul1-5 but are considered atypical cullins. Each cullin-RING complex recognizes it specific substrates through a group of substrate recruitment proteins. For example, Cul1 has more than 60 substrate recognition partners called F-box proteins, which can interact with the Cul1 adaptor Skp1 through F-box and recruit the substrates using another motif. The Skp1-Cul1-F-box complex is also named as SCF. Cul2 and Cul5 share a common adaptor complex consisting of Elongin C, which has sequence homology with Skp1, and Elongin B. A family of substrate receptors called BC-box containing proteins, including the von Hippel Lindau (VHL) tumor suppressor and suppressor of cytokine signaling (SOCS) proteins, are recruited to Cul2 or Cul5 through interacting with Elongin BC. Both Skp1 and Elongin C have a Bric-a-Brac, Tramtrack, and Broad complex (BTB) fold to interact with the N-terminus of cullins. However, Cul4A utilizes a different type of adaptor protein called the damaged DNA binding protein 1 (DDB1), which lacks the BTB fold. Instead, DDB1 contains three distinct WD40-like β-propeller domains, BPA, BPB and BPC. DDB1 is docked on the N-terminus of Cul4A through BPB, while BPA and BPC form a symmetrical double propeller pointing away from the cullin and bind to the CRL4 substrate receptors, DCAFs (DDB1 and Cul4 associated factors) or DWDs (DDB1-binding WD40 proteins). Distinct from all the other cullins, CRL3s integrate the function of cullin binding and substrate recognition into one single polypeptide. A group of BTB-domain containing proteins were found to interact with Cul3 through the BTB fold and recruit the substrates using another module (Xu, et. al., 2003). There are more than 200 different BTB genes in human genome but only about 60 were reported to be potential Cul3 adaptors (Bennett, et. al., 2010). In mouse embryonic stem cells, I have identified 31 BTB proteins that bind Cul3, with 18 BTB-Kelch repeat proteins, 4 potassium-channel-tetramerization-domain-containing proteins and 8 proteins with other substrate recognition motifs.

A recent study of $CRL3^{SPOP}$ revealed that the Cul3 adaptor SPOP forms a homodimer through BTB domain thereby providing two substrate recognition motifs and bringing together two catalytic cores (Zhuang, et. al., 2009). The dual substrate recognition greatly enhances the binding affinity of the substrates as SPOP dimerization mutants ubiquitinate its substrates much more inefficiently. Studies of another well-characterized BTB protein, Keap1, provide additional evidence of how BTB dimerization is required for effective substrate targeting. Keap1 is a Kelch-repeat-containing BTB protein that mediates the constitutive turnover of the transcription factor Nrf2 by Cul3. There is a rich body of evidence showing that two distinct degrons exist on Nrf2, which bind two different Kelch monomers. And Keap1 can only ubiquitinate Nrf2 when both degrons are present. However, it is not known whether heterodimerization of different BTB proteins exist in vivo although such interaction has been observed in our co-IP experiment and in-vitro binding experiment. It will largely increase the substrate spectrum if BTB heterodimerization is physiologically relevant.

In this chapter, I will discuss the isolation of Cul3-interacting BTB proteins in mouse ES cell extract, characterization of BTB dimerization, and in particular, the identification of Klhl12 as the ESC-specific Cul3 adaptor.

3.2 Results

3.2.1 Isolation of Cul3-Interacting BTB-Domain Containing Proteins in Mouse ES Cells

Like other members of Cullin family, Cul3 ubiquitinates the substrates through its specific substrate adaptors (Fig. 3-1A). It was first reported in *C. elegans* that a group of proteins containing BTB/POZ domain interact with Cul3 in a yeast two-hybrid screen (Xu, et. al., 2003). This domain, which was initially identified in the *Drosophila* transcriptional repressors *broad complex*, *tramtrack and bric-a-brac*, is present in more than 120 C. elegans and 190 human proteins (Collins, et. al., 2001). Interestingly, Skp1 and BTB domain adopt similar three-dimensional α/β structures (Schulman, et. al., 2000; Aravind, et. al., 1999), indicating structural conservation of interaction with cullins.

To identify BTB-domain containing proteins that interact with Cul3 in mouse ES cells, I used purified recombinant Cul3-3xFLAG as bait and incubated with mouse ES cell extract. IP samples were run on SDS-PAGE gel for commassie staining, and specific bands were cut out and sent for mass spec analysis (Fig. 3-1B). Among the 31 BTB proteins identified, 18 of them have kelch-like-repeats in addition to BTB/POZ domain, and 4 contain potassium channel tetramerization domain. Other potential substrate recognition domains are RCC1 domain, Ras-like domain, PHR domain and etc. (Table S2).

To confirm the interaction of these BTB proteins with Cul3, I performed co-IP experiment in 293T cells by transiently express both FLAG-tagged Cul3 and myc-tagged BTB proteins. Cells lysates were subject of FLAG IP and interaction was detected by western blotting against myc. Indeed, all of the BTB proteins identified directly interact with Cul3 (Fig. 3-1C, data not shown).

Structural studies of SCF complex revealed that Cul1 interact with Skp1 through Helix2 and Helix5 of its first N-terminal cullin repeat (Zheng, et. al., 2002). Cul3 shares structural homology with Cul1 with highly conserved N-terminal H2 and H5. To examine whether the corresponding residues on Cul3 are also involved in BTB interaction, we generated Cul3 mutants in H2 (L52A, E55A, Y58A, R59A, Y62A), or H5 (Y125A, R128A) or both, and tested their ability to pulldown BTB proteins in coIP experiment of 293T cells. Interestingly, some BTB proteins like KBTBD8 primarily interact with H2 of Cul3, whereas for others like Klhl12, residues of both H2 and H5 on Cul3 are involved in binding (Fig. 3-1D, data not shown).

3.2.2 Characterization of BTB Dimerization

BTB proteins dimerize with each other through hydrophobic interaction in BTB domain, which is independent of the Cul3 binding site (Zhuang, et. al., 2009). And this dimerization has been shown to be important for enhancing substrate binding affinity and efficient ubiquitination by several BTB proteins like SPOP and Keap1. To examine whether dimerization is a common feature of other BTB proteins identified in our IP, I co-expressed one FLAG-tagged BTB protein as bait and an array of other myc-tagged BTB proteins as preys in 293T cells, and performed FLAG IP. Interestingly, from all the BTBs tested as bait (Klhl9, Klhl12, Klhl22, Klhl25, and KBTBD8), I found that BTB proteins can always form homodimers with themselves. In addition, structurally related BTB proteins can form heterodimers with each other, e.g. Klhl9 with Klhl13. However, whether such heterodimerization is physiologically relevant remains to be confirmed. The dimerization pattern of BTB proteins show that the structural symmetry of the BTB domain is important for the hydrophobic interaction to occur.

3.2.3 Identification of Klhl12 as ESC-Specific Cul3 Adaptor

Simple RNAi screen against BTB genes in mouse ES cells did not reproduce the Cul3 phenotype (data not shown). This could be due to BTB dimerization, or several BTB proteins involved in the same pathway, or simply incomplete depletion by siRNA. To isolate BTB genes specifically important for Cul3 function in ES cells, I made use of the observation that important stem cell regulators are usually highly expressed in stem cell state and down-regulated during differentiation. Based on this fact, I examined the expression of BTB genes during ES cell differentiation to embryoid bodies. Among the 31 BTB genes, the mRNA levels of Klhl12 and KBTBD8 decrease significantly together with Oct4 and Nanog, the two master regulators for ES cells, indicating the potential significance of these two BTB genes in ES cell regulation (Fig. 3-3A). The up-regulated BTB genes include Klhl9 and Klhl13, which have been shown to be important for mitosis in somatic cells (Sumara, et. al., 2007). The down-regulation of Klhl12 and up-regulation of Klhl13 were confirmed respectively by using specific antibodies in western blot (Fig. 3-3B). Interestingly, the active neddylated form of Cul3 is highly enriched in the ESC state, indicating its important role in ES cells.

To test whether Klhl12 and KBTBD8 also function in the Integrin-Src-Rac-Actin pathway, mouse ES cells transfected with scramble siRNA, siKlhl12 or siKBTBD8 were treated with an increasing concentration of dasatinib, the Src kinase inhibitor. Only depletion of Klhl12 but not KBTBD8 has a synthetic lethal effect with dasatinib and causes cell compaction, the same phenotype upon Cul3 depletion (Fig. 3-3C, 3-3E). This led us to the conclusion that Klhl12 is the BTB gene important for Cul3 function in mouse ES cells by acting in the Integrin pathway. To confirm direct interaction between Cul3 and Klhl12, I precipitated endogenous Cul3 using specific antibody from mouse ES cell extract and detected Klhl12 protein (Fig. 3-3D). Indeed, substantial amount of endogenous Klhl12 is associated with Cul3.

3.3 Discussion

Combining biochemical assay and gene expression analysis, I have identified Klhl12 as the ES cell-specific Cul3 adaptor. Klhl12 interacts with Cul3 through the BTB domain, which shares a similar α/β fold with Skp1. It has been reported that Skp1 contacts Cul1 through several residues located in β-strand 3 (S3) and in α-helix 5 (H5) (Zheng, et. al., 2002). It will be interesting to generate mutants of corresponding sites on Klhl12 in order to fully understand how the Cul3-Klhl12 interaction occurs. Like other Kelch-like proteins, the BTB domain of Klhl12 is followed by a BACK domain (BTB and C-terminal Kelch domain). The BACK domain may also be involved in Cul3 interaction since it contains a '3-box', a required element in Cul3 recognition (Zhuang, et. al., 2009). This explains why all BTB and Kelch-like proteins are Cul3 adaptors. Co-IP experiment in 293T cells shows that Klhl12 can form heterodimers with other BTB proteins as well as homodimer. However, mass spec data from Klhl12 stable cell line only yields a few peptides of Klhl21 and Klhl26 (data not shown), raising suspicion on the physiological relevance of heterodimers. One explanation could be that Klhl12 homodimer is the dominant form in vivo whereas a small fraction of Klhl12 also forms heterodimer with other BTB proteins and target different substrates. Depletion of Klhl12 causes cell compaction together with low concentration of dasatinib, indicating that Klhl12 also functions in the integrin pathway. However, the exact function of $Cul3^{Klhl12}$ in ES cells remains unknown until the identification of their substrate(s), which I will discuss in the following chapters.

3.4 Material and Methods

Plasmids and Antibodies

Human Cul3 and Klhl12 were cloned into pcDNA4 and pcDNA5 vectors for expression of recombinant FLAG-tagged proteins in mammalian cells. Human BTB genes were also cloned into pCS2-7xmyc vector for expression in mammalian cells. Cul3-3xFLAG-6xHis was cloned into pFastBac vector and expressed in SF9 insect cells using the Bac-to-Bac baculovirus expression system of Invitrogen and purified by Ni-NTA agarose.

Klhl12 and Klhl13 mouse monoclonal antibodies were raised against 205-466aa of human Klhl12 and 325-655aa of human Klhl13. Both antibodies are available commercially at Promab Biotechnologies, cat. #30058 and #30067. Cul3 antibody is from Bethyl Laboratories (cat. # A301-109A)

Identification of Cul3-Interacting BTB Proteins in Mouse ES cells

Fifty 15cm plates of D3 mouse ES cell were grown as previously described. Cell extract was prepared by freeze-thaw twice in 5ml lysis buffer (20mM HEPES buffer pH7.5, 5mM KCl, 1.5mM MgCl2, protease inhibitor) and supplemented with 150mM NaCl and 0.1% NP40 prior to IP. 800ul of recombinant Cul3-3xFLAG-6xHis purified from insect cells was conjugated to 60ul of FLAG M2 affinity resin (Sigma, cat. # A2220-5ML) and incubated with 5ml pre-cleared ES cell extract for 4hrs at 4C. After extensive washing, FLAG beads were boiled in 100ul SDS-containing gel loading buffer. The eluted proteins were loaded on a SDS-PAGE gel and subject to commassie staining. Specific gel bands were cut out and sent for mass spec analysis. As control, unconjugated FLAG beads was incubated with ES cells extract and treated in a same way.

Co-IP Experiment in 293T Cells

293T cells were seeded at 80,000/well in 12-well plate and transfection was performed when the cell density reached about 30-40%. FLAG-tagged and Myc-tagged genes were co-transfected using Transit Mirus 293T. 48 hours post transfection, cells were harvested and lysed by freeze-thaw in hypotonic lysis buffer, and supplemented with 150mM NaCl and 0.1% NP40. To perform IP, FLAG resins were added to each reaction and incubated for 3-4hrs at 4C. After extensive washing, the FLAG resins were boiled in gel loading buffer and loaded on SDS-PAGE gel for western blot analysis.

Immunoprecipitation of Endogenous Protein Complexes

To confirm the interaction of endogenous proteins, D3 mouse ES cells were lysed by freeze-thaw in hypotonic lysis buffer. Pre-immune rabbit antibody or specific antibody against Cul3 were conjugated to protein G agarose beads respectively and added to the cleared cell lysate supplemented with 150mM NaCl and 0.1% NP40, and incubated at 4C for 4 hours. The protein complexes were eluted by adding gel-loading buffer containing SDS and boiling. The presence of endogenous proteins in the complex was detected by western blot using antibody against Klhl12.

Differentiation of ES Cells into Embryoid Bodies

To differentiate mouse ES cells into embryoid bodies, the undifferentiated D3 mouse ES cells were trypsinized, washed once with LIF-free ESC media, and seeded at $2x10^6$ cells/dish onto 10-cm Corning Ultra-Low-Attachment Dishes (Corning cat. # 3262) containing 10 ml of ESC medium without LIF. After 24 hours, the cells were dissociated from the plate by gentle pipetting of the medium and collected in a 15ml Falcon tube by centrifugation. The supernatant was aspirated off and the cells were re-seeded onto 10-cm Corning Ultra-Low-Attachment Dishes containing fresh ESC medium without LIF. Continue to culture the EBs and change medium every other day. The ES cells and EBs samples were collected on Day 0, Day 6 and Day 9 after differentiation for RT-qPCR and western blot analysis.

Table S2. List of Cul3-interacting BTB proteins in mouse ES cells

Name	Substrate binding domain
BTBD1	PHR domain
BTBD2	PHR domain
BTBD9	
ibtk	RCC1 domain
Rcbtb1	RCC1 domain
RHOBTB3	Ras-like domain
zbtb11	zinc finger domain
lpp	
Ivns1abp	
KCTD2	potassium channel tetramerisation domain
KCTD3	potassium channel tetramerisation domain
KCTD9	potassium channel tetramerisation domain
KCTD10	potassium channel tetramerisation domain
KBTBD2	Kelch-like repeats
KBTBD4	Kelch-like repeats
KBTBD8	Kelch-like repeats
klhdc5	Kelch-like repeats
enc1	Kelch-like repeats
klhl12	Kelch-like repeats
klhl13	Kelch-like repeats
klhl18	Kelch-like repeats
klhl2	Kelch-like repeats
klhl20	Kelch-like repeats
klhl21	Kelch-like repeats
klhl22	Kelch-like repeats
klhl24	Kelch-like repeats
klhl25	Kelch-like repeats
klhl26	Kelch-like repeats
klhl3	Kelch-like repeats
klhl8	Kelch-like repeats
klhl9	Kelch-like repeats

Fig. 3-1: Identification of Cul3-interacting BTB proteins in mouse ES cells

(A) Cul3 ubiquitinates its substrates by interacting with a group of BTB-domain-containing substrate adaptor proteins.

(B) IP of Cul3-interacting BTB proteins from mouse ES cell extract. Recombinant Flag-tagged Cul3 protein was purified from insect cells, conjugated to FLAG beads, and incubated with mouse ES cell extract. IP samples were run on SDS PAGE gel and specific gel bands were cut out and sent for mass spec analysis.

(C) Cul3 directly interacts with the BTB proteins identified by mass spec. Myc-BTB proteins were transfected in the presence or absence of FLAG-Cul3 in 293T cells. Cell lysates were subject to anti-FLAG IP and interaction was detected using anti-myc antibody in western blot.

(D) H2 and H5 of Cul3 N-terminus are important for BTB binding. Myc-Klhl12 or Myc-KBTBD8 were co-transfected with FLAG-tagged Cul3 mutants in 293T cells. Cell lysates were subject to anti-FLAG IP and interaction was detected using anti-myc antibody in western blot.

A

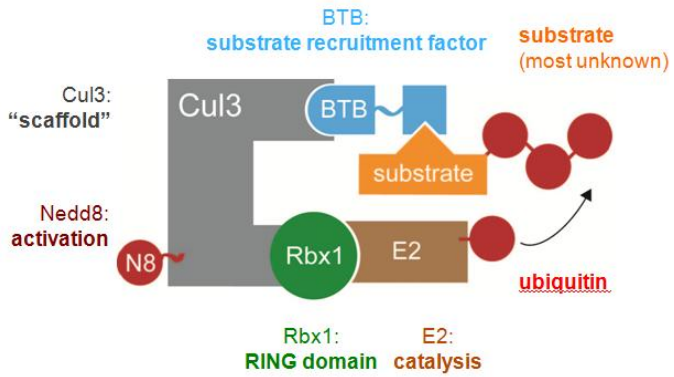
BTB:
substrate recruitment factor
substrate
(most unknown)
Cul3:
"scaffold"
Cul3
BTB
substrate
Nedd8:
activation
N8
Rbx1
E2
ubiquitin
Rbx1:
RING domain
E2:
catalysis

B

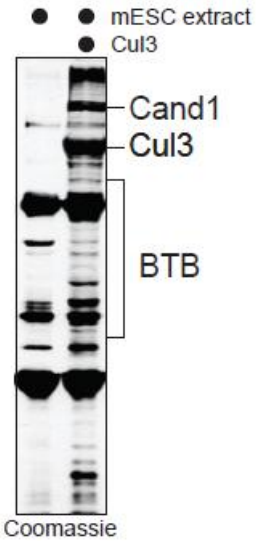
mESC extract
Cul3
Cand1
Cul3
BTB
Coomassie

C

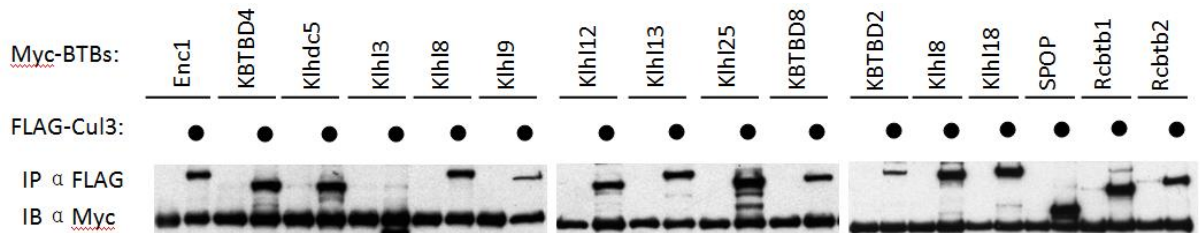
Myc-BTBs:
Enc1
KBTBD4
Klhdc5
Klhl3
Klhl8
Klhl9
Klhl12
Klhl13
Klhl25
KBTBD8
KBTBD2
Klhl8
Klhl18
SPOP
Rcbtb1
Rcbtb2
FLAG-Cul3:
IP α FLAG
IB α Myc

D

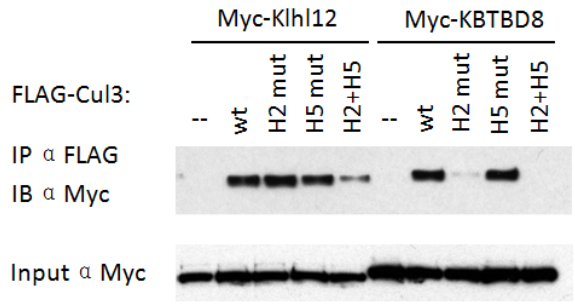
Myc-Klhl12
Myc-KBTBD8
FLAG-Cul3:
--
wt
H2 mut
H5 mut
H2+H5
--
wt
H2 mut
H5 mut
H2+H5
IP α FLAG
IB α Myc
Input α Myc

Fig. 3-2: Dimerization of BTB proteins

Dimerization of BTB proteins were tested in a co-IP experiment. An array of myc-tagged BTB proteins were co-expressed in the presence or absence of FLAG-tagged bait proteins, Klhl9 (A), Klhl12 (B), Klhl22 (C), Klhl25 (D), and KBTBD8 (E) in 293T cells. Cell lysates were subject to FLAG IP and interaction was detected using α-myc antibody in western blot.

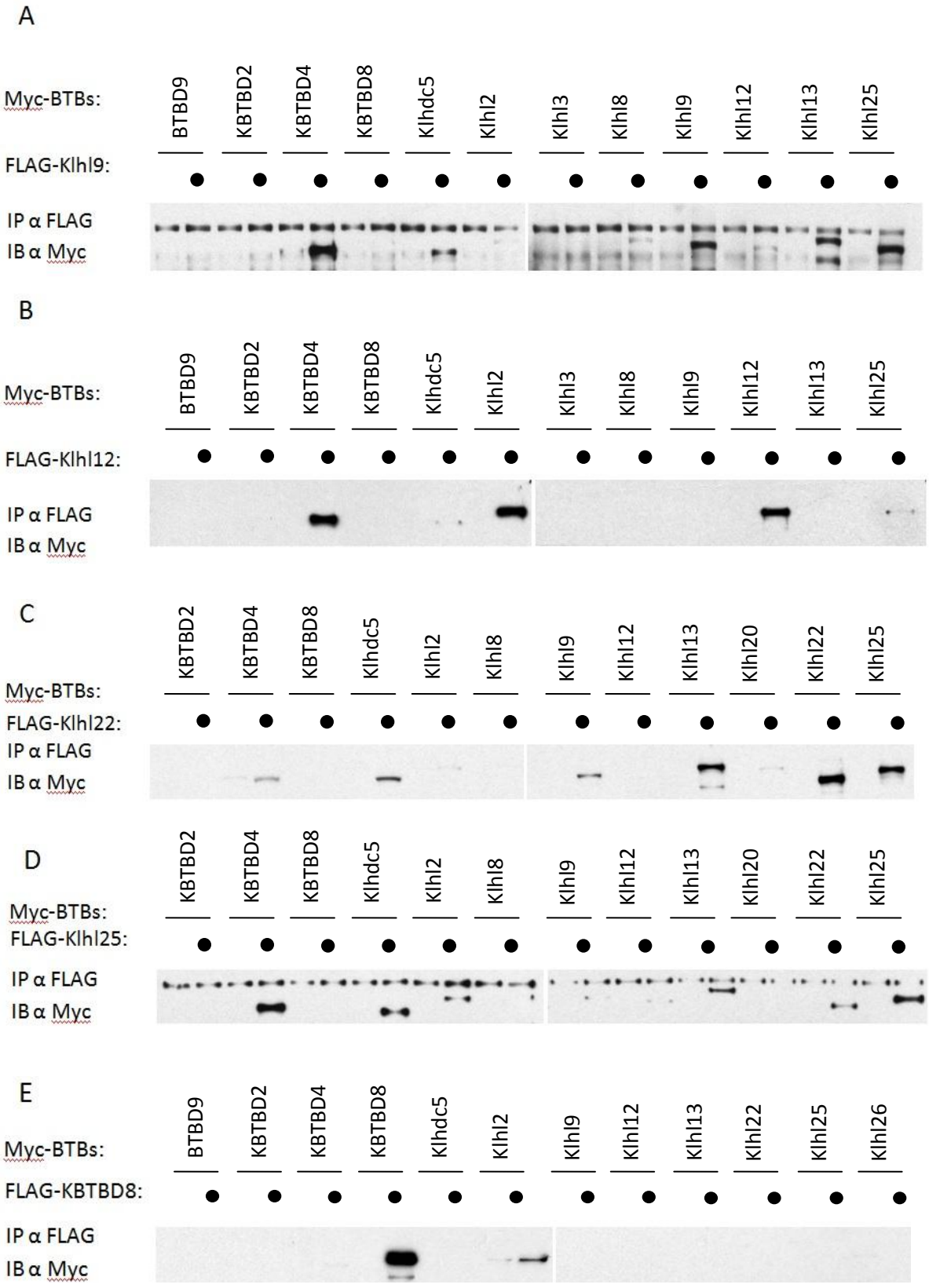
A
Myc-BTBs:
BTBD9
KBTBD2
KBTBD4
KBTBD8
Klhdc5
Klhl2
Klhl3
Klhl8
Klhl9
Klhl12
Klhl13
Klhl25
FLAG-Klhl9:
IP α FLAG
IB α Myc
B
Myc-BTBs:
BTBD9
KBTBD2
KBTBD4
KBTBD8
Klhdc5
Klhl2
Klhl3
Klhl8
Klhl9
Klhl12
Klhl13
Klhl25
FLAG-Klhl12:
IP α FLAG
IB α Myc
C
Myc-BTBs:
KBTBD2
KBTBD4
KBTBD8
Klhdc5
Klhl2
Klhl8
Klhl9
Klhl12
Klhl13
Klhl20
Klhl22
Klhl25
FLAG-Klhl22:
IP α FLAG
IB α Myc
D
Myc-BTBs:
KBTBD2
KBTBD4
KBTBD8
Klhdc5
Klhl2
Klhl8
Klhl9
Klhl12
Klhl13
Klhl20
Klhl22
Klhl25
FLAG-Klhl25:
IP α FLAG
IB α Myc
E
Myc-BTBs:
BTBD9
KBTBD2
KBTBD4
KBTBD8
Klhdc5
Klhl2
Klhl9
Klhl12
Klhl13
Klhl22
Klhl25
Klhl26
FLAG-KBTBD8:
IP α FLAG
IB α Myc

Fig. 3-3: Identification of Klhl12 as the ESC-specific Cul3 adaptor

(A) Klhl12 and KBTBD8 are down-regulated upon ES cell differentiation. Mouse ES cells were differentiated into embryoid bodies and the expression of BTB genes was analyzed by quantitative real-time PCR.

(B) Klhl12 down-regulation upon ES cell differentiation is confirmed by western blot. Mouse ES cells were differentiated into embryoid bodies and the protein level of Klhl12 is analyzed using specific antibody against it. The expression of Klhl12 is co-regulated with Oct4, a key player in ES cells.

(C) Depletion of Klhl12 but not KBTBD8 causes cell compaction phenotype in the presence of 50nM dasatinib. Mouse ES cells were treated with scramble siRNA, siKlhl12 or siKBTBD8 together with 50nM dasatinib. Cell morphology was examined under light microscopy and confocal microscopy.

(D) Endogenous Klhl12 interacts with Cul3. Mouse ES cell lysate was subject to immunoprecipitation by specific Cul3 antibody. Endogenous Klhl12 was co-purified in the complex as determined by western blot. Input represents 10% of total lysate.

(E) Depletion of Klhl12 causes cell compaction phenotype with increasing concentration of dasatinib.

A

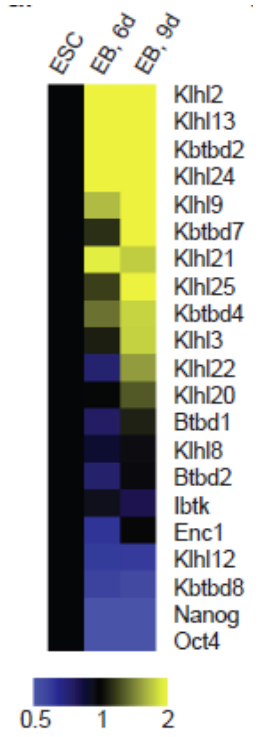
ESC
EB, 6d
EB, 9d
Klhl2
Klhl13
Kbtbd2
Klhl24
Klhl9
Kbtbd7
Klhl21
Klhl25
Kbtbd4
Klhl3
Klhl22
Klhl20
Btbd1
Klhl8
Btbd2
Ibtk
Enc1
Klhl12
Kbtbd8
Nanog
Oct4
0.5
1
2

B

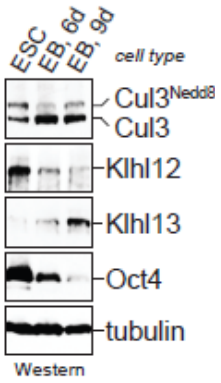
ESC
EB, 6d
EB, 9d
cell type
Cul3Nedd8
Cul3
Klhl12
Klhl13
Oct4
tubulin
Western

C

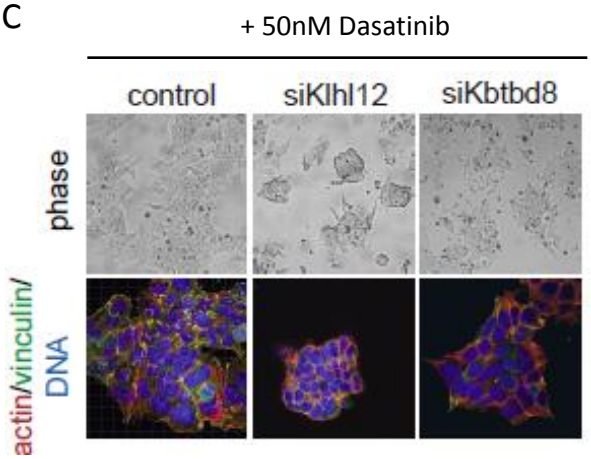
+ 50nM Dasatinib
control
siKlhl12
siKbtbd8
phase
actin/vinculin/
DNA

D

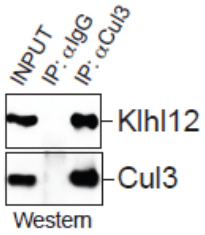
INPUT
IP: αIgG
IP: αCul3
Klhl12
Cul3
Western

E

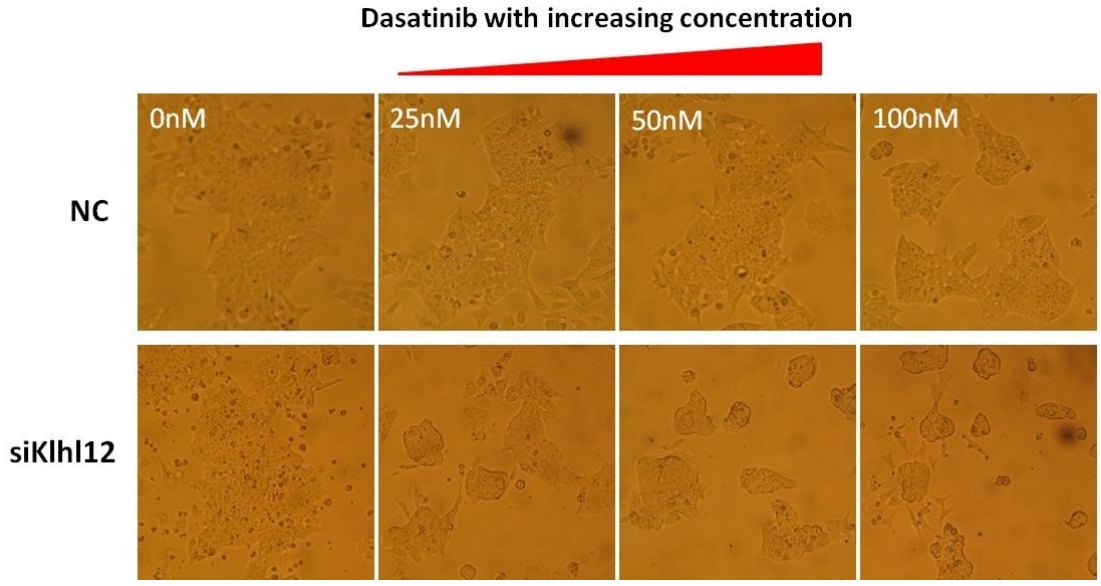
Dasatinib with increasing concentration
0nM
25nM
50nM
100nM
NC
siKlhl12

Chapter Four

Identification of COPII Protein Sec31A as $Cul3^{Klhl12}$ Substrate

4.1 Introduction

In this chapter, I will discuss the identification and characterization of COPII coat protein Sec31A as the major ubiquitination target of $Cul3^{Klhl12}$. Cargo proteins enter the secretary pathway from the endoplasmic reticulum (ER) in membrane-bound vesicles coated with the COPII complex (coat protein II), which consists of five proteins, Sar1 GTPase, Sec23/24 heterodimer, and Sec13/31 heterotetramer (Lee, et. al., 2004). In yeast, these vesicles travel directly to Golgi where the cargo proteins undergo further modification and sorting. In mammalian cells, however, these vesicles first traffic to an intermediate structure called ERGIC (the ER-Golgi intermediate compartment), where additional sorting occurs before the proteins are trafficked to the Golgi (Presley, et. al., 1997; Scales, et. al., 1997; Martinez-Menarguez, et. al., 1999). The COPII protein complex is not only required for vesicle budding from ER, but also provides structural roles and cargo selectivity. The vesicle budding is initiated by Sar1, which is stimulated by Sec12 from an inactive GDP-bound form to an active GTP-bound form (Yoshihisa T, et. al., 1993; Barlowe, et. al., 1993). The Sar1-GTP can cause the curvature of ER membrane and recruits the Sec23/24 heterodimer, which further binds to Sec13/31 complex. The Sec13/31 heterotetramer then oligomerize and assemble into a cuboctahedral cage with a diameter of ~80nm and the vesicle is budded off the membrane (Lederkremer, et. al., 2001; Sato, et. al., 2005).

In mammalian cells, there are two known isoforms of Sar1, two of Sec23, four of Sec24 and two of Sec31. The size of COPII vesicles is largely determined by outer layer formed by Sec13/31. Structural studies have shown that this outer layer consists of 24 Sec13/31 heterotetramers with two Sec31s forming homodimer and two Sec13s binding close to the N-terminus of Sec31. At each vertex, the N-terminal WD-40 domains from four different Sec31 interact with each other and the angles of interaction determine the shape and size of the COPII cage (Stagg, et. al., 2006; Fath, et. al., 2007; Stagg, et. al., 2008).

We have proved that Klhl12 stably associates with Sec31A in vivo and causes the mono-ubiquitination of Sec31A at a flexible lysine site. The identification of Sec31A as $Cul3^{Klhl12}$ target revealed a novel regulation of COPII-mediated trafficking pathway. The mechanism of this regulation and its significant function in mouse ES cells will be further discussed in the following chapter.

4.2 Results

4.2.1 Identification of Sec31A as an interacting partner for Klhl12

In order to fully understand $Cul3^{Klhl12}$ function, I used the biochemical assays with mass spec analysis to isolate potential $Cul3^{Klhl12}$ substrate(s). Inducible 293T stable cell lines expressing either of FLAG-tagged Klhl9, Klhl12 or KBTBD8 were subject to FLAG IP and specific interacting proteins were identified by mass spec. Interestingly, I found substantial amount of Sec13/31A complex in the FLAG eluate when Klhl12 but not the other two BTB proteins was used as the bait (Fig. 4-1A, 4-1B). To test whether endogenous Klhl12 and Sec13/31A also associate with each other, specific antibody against Sec13 was used to pull down

endogenous Sec13/31A complex from either mouse ES cell or Hela cell extract. More than 15% of endogenous Klhl12 comes down with Sec13/31A (Fig. 4-1C). The colocalization of Klhl12 with Sec13/31A at ERES (ER-exit site) was also observed in immunofluorescence staining (Fig. 4-1D). To exclude the possibility that Sec13/31A may associate with Klhl12 through some intermediate binding partners, purified Sec13/31A complex was incubated together with recombinant MBP-tagged BTB proteins conjugated to amylose resins and the direct interaction was detected by western blot. Only MBP-Klhl12 but not other BTB proteins can pull down Sec13/31A (Fig. 4-1E). Sec13 and Sec31A form stable complex with each other in vitro and in vivo. To distinguish which component is the direct binding partner for Klhl12, I synthesized Sec13 and Sec31A independently using an in-vitro transcription/translation system (IVT), and tested their ability to bind recombinant MBP-Klhl12. Sec31A but not Sec13 directly interacts with Klhl12 (Fig. 4-1F).

Klhl12 is a member of kelch repeat superfamily with an N-terminal BTB/POZ domain. The kelch repeat domain is usually a set of six kelch motifs collectively forming a β-propeller structure. Each kelch motif is a segment of 44-56 amino acids with several conserved hydrophobic residues, a double glycine element and two characteristically spaced aromatic residues. It forms a four-stranded β-sheet corresponding to a single blade of the propeller (Fig. 4-2A; Adams et. al., 2000). The loop sequences linking β2/β3 strands, and β4/β1 strands are relatively flexible and divergent among different kelch-like proteins. They are involved in substrate recognition for KEAP1. To identify the key residues on Klhl12 for Sec31A binding, we did a mutation screening of residues within these flexible loops. We found that $Klhl12^{FG289AA}$, $Klhl12^{RGL369AAA}$, $Klhl12^{YDG434AAA}$ and $Klhl12^{RCY510AAA}$ are defective in binding Sec31A but not Cul3 (Fig. 4-2B). These residues cluster around the top side of the Kelch propeller, which KEAP1 uses to interact with its substrate Nrf2.

On the side of Sec31A, we found residue 370-390 is required for Klhl12 interaction (Fig. 4-2C). This region is a flexible linker between the N-terminal WD40 domain and Sec13 binding site, which provides an easy access for Klhl12 recognition.

4.2.2 Mono-ubiquitination of Sec31A by $Cul3^{Klhl12}$

To test whether Sec31A is a ubiquitination substrate of $Cul3^{Klhl12}$, I set up the in-vitro ubiquitination assay using recombinantly purified $Cul3^{Klhl12}$ and Sec13/31A. Indeed, a single shifted band corresponding to mono-ubiquitinated Sec31A was present when ubiquitin was added to the reaction (Fig. 4-3A). This modification of Sec31A was dependant on Klhl12-Sec31A interaction as the binding-deficient mutant of $Klhl12^{FG289AA}$ was unable to catalyze the reaction (Fig. 4-3B). Then I tested whether Sec31A is a ubiquitination substrate of $Cul3^{Klhl12}$ in vivo using the His-ubiquitin pulldown assay in 293T cells (Fig. 4-3C). Sec31A was modified with a single ubiquitin under physiological condition when no exogenous Cul3 or Klhl12 was overexpressed. Upon expression of Klhl12 and Cul3, higher-molecular-weight species of Sec31A were greatly enhanced. These modified species represent polyubiquitinated Sec31A as they totally disappear when the lysine-free His-ubiquitin unable to assemble polyubiquitination chains was transfected. The mono-ubiquitination of Sec31A in vivo is also dependant on $Cul3^{Klhl12}$ since the overexpression of truncated Cul3 (Fig. 4-3C) or the depletion of Cul3 and

Klhl12 by RNAi (Fig. 4-3D) both abolishes the modification. In addition, the overexpression of Klhl12 mutants unable to bind Sec31A inhibits its ubiquitination presumably by sequestering endogenous Cul3 or Klhl12 (Fig. 4-3E).

The overexpression of $Cul3^{Klhl12}$ causes polyubiquitination and degradation of Sec31A (Fig. 4-3C, 4-3F). However, under physiological conditions, Sec31A is only mono-ubiquitinated instead of poly-ubiquitinated since the depletion of $Cul3^{Klhl12}$ or treatment with MG132 does not lead to Sec31A stabilization (Fig. 4-3G).

4.3 Discussion

Klhl12 belongs to the family of Kelch-repeat and BTB-domain-containing protein. It is composed of an N-terminal BTB-BACK domain responsible for Cul3 interaction and dimerization, a flexible linker followed by the C-terminal β-propeller structures usually made of six Kelch repeats. The loop regions between β2/β3 and β4/β1 strands of each Kelch repeat are highly divergent among different Kelch-like proteins, and are believed to confer substrate specificity during interaction. In addition to the Kelch domain, dimerization of Klhl12 through BTB/BACK domain is also required for substrate binding since Kelch domain of Klhl12 alone fails to pull down Sec31A in an in vitro MBP binding assay, nor does it colocalize with Sec31A at ERES in IF staining (data not shown). This raises the possibility that Klhl12 binds Sec31A through two recognition motifs. There is possibly a cryptic recognition site on Sec31A in addition to the major binding site so that Klhl12 and Sec31A form a 2:1 complex as in the case of Keap1-Nrf2 interaction (McMahon, et. al., 2006; Tong, et. al., 2006). Alternatively, two Klhl12 molecules can bind to the same site of two individual Sec31A in the COPII coat. Further biophysical assays like analytical ultracentrifugation (AUC), surface plasmon resonance (SPR) and NMR are required to determine the mode of interaction between Klhl12 and Sec31.

Our data has shown that the interaction between Klhl12 and Sec31A is strong and stable compared with other E3-substrate recognition, and a significant portion of endogenous Klhl12 associates with Sec31A. However, the modification of Sec31A by $Cul3^{Klhl12}$ is only limited to mono-ubiquitination and in vivo, only a very small fraction of Sec31A is being ubiquitinated. Identification of additional players in Sec31A ubiquitination will shed light on how this modification is regulated. It is possible that $Cul3^{Klhl12}$ adds the first ubiquitin on Sec31A whereas another BTB protein elongates the ubiquitin chain. Or a deubiquitinase (DUB) exists in the complex which removes the ubiquitin from Sec31A and provides timely regulation of the modification.

4.4 Material and Methods

Identification of Klhl12 Binding Partners from Inducible Stable 293T Cells

To make the doxycycline-inducible 293T cell lines stably expressing different BTB proteins, Klhl9, Klhl12 and KBTBD8 were cloned into pCDNA5 vector with a C-terminal 3xFLAG tag. The plasmids were transfected into Flp-In™ T-REx™ 293 Cell Line from Invitrogen and the

stable cell lines were isolated as instructed. The expression of different BTB proteins was induced by adding 1ug/ml doxycycline to the cells grown in fifty 15cm plates. 48 hours post induction, cells were harvested and lysed by douncing in hypotonic buffer plus 0.1%NP40. The cleared cell extract were subject to FLAG IP and specific binding proteins were eluted with FLAG peptide. Samples were loaded onto SDS-PAGE gel and analyzed by mass spectrometry.

In-vitro Protein Interaction Assay

To define the binding domains of Klhl12 and Sec31A interaction, 20ug each of recombinant MBP-Klhl12 protein, various mutants and MBP as control were coupled to 15ul amylose resin by incubating at 4C for 1 hour. Cul3, Sec31A and its mutants were expressed from a pCS2 vector and labeled with S-35 Methionine using an in-vitro transcription/translation system (TnT Sp6 Quick Coupled Trsnc/trans Syst, Promega, cat. # L2080). The radioactively labeled Cul3 or Sec31A were then incubated with recombinant MBP-Klhl12 protein or its mutants on beads at 4C for 3 hours. The beads were washed 4x with TBST and 2x with TBS, and boiled in SDS gel loading buffer. The samples were run on a SDS-PAGE gel and the results were visualized by autoradiography.

In-vitro Ubiquitination of Sec31A by $Cul3^{Klhl12}$

Cul3/Rbx1 was conjugated to NEDD8 at 30C for 1hr with the following conditions: 2.5 mM Tris/HCl pH 7.5, 5 mM NaCl, 1 mM MgCl2, 1 mM DTT, 1x energy mix, 1uM APPBP1-UBA3, 1.2 uM Ubc12, 4 uM Cul3/Rbx1, and 60 uM NEDD8. For in-vitro ubiquitination of Sec31A, we set up a 10ul reaction as follows: 2.5 mM Tris/HCl pH 7.5, 5 mM NaCl, 1 mM MgCl2, 1 mM DTT, 1x energy mix, 100nM UBA1, 1uM UbcH5c, 1uM Cul3~Nedd8/Rbx1, 1uM Klhl12, 150uM ubiquitin, 0.05ug Sec13/31A. The reaction was carried out at 30C for 1hr and stopped by adding SDS gel loading buffer.

In-vivo Ubiquitination Assays in 293T Cells

For in-vivo ubiquitination assay, pCS2-HA-Sec13/31A was co-transfected with or without pCS2-His-ubiquitin, pcDNA5-Klhl12-FLAG, and pcDNA4-Cul3-FLAG or pcDNA4-Cul3N250-FLAG into 293T cells grown in 10-cm TC dish with Calsium Phosphate transfection. 48 hours later, cells were harvested with gentle scraping and resuspended in 1ml buffer A (6M guanidine chloride, 0.1 M Na2HPO4/NaH2PO4 and 10mM immidazole,pH 8.0). The cells were lysed by sonication for 10s, incubated with 25ul Ni-NTA agarose at room temperature for 3 hours. The beads were washed 2x with buffer A, 2x with buffer A/TI (1 volume buffer A and 3 volumes buffer TI), 1x with buffer TI (25 mM Tris-Cl, 20 mM imidazole, pH6.8), and boiled in 60ul SDS gel loading buffer containing 300mM imidazole and 50mM β ME. Samples were loaded onto SDS-PAGE gel and the ubiquitinated Sec31A was detected by western blot using antibody against Sec31A.

To detect Sec31A ubiquitination upon Cul3/Klhl12 depletion, siRNA oligos against Cul3 or Klhl12 were co-transfected with pCS2-HA-Sec13/31A and pCS2-His-ubiquitin using Calsium Phosphate at a final concentration of 100nM oligos. Similarly, the Ni-NTA IP was performed 48 hours post transfection and Sec31A ubiquitination was detected by western blot.

Fig. 4-1: Sec31A is the interacting partner for Klhl12

(A) Sec13/31A was identified as specific binding partner for Klhl12 but not Klhl9. Inducible 293T stable cell lines expressing either FLAG-tagged Klhl9 or Klhl12 were subject to FLAG IP. The IP eluate was run on a SDS-PAGE gel and specific binding proteins were identified by mass spec analysis.

(B) The interaction of Sec13/31A with $Klhl12^{FLAG}$ was confirmed by western blot. IP samples from 293T stable cell lines of $Klhl9^{FLAG}$, $Klhl12^{FLAG}$, or $KBTBD8^{FLAG}$ were run on a gel and the presence of Sec13 and Sec31A was detected by western blot.

(C) Endogenous Klhl12 associates with Sec13/31A complex. Mouse ES cell extract was subject to immunoprecipitation using either pre-immune IgG or specific antibody against Sec13. The association of endogenous Klhl12 was detected by western blot.

(D) Immunofluorescence staining of Hela cells showed that endogenous Klhl12 colocalizes with Sec13 at ER-exit site (ERES).

(E) Sec13/31A interacts with Klhl12 in vitro. Purified Sec13/31A complex was incubated with MBP-BTBs coupled on amylose resins. Only MBP-Klhl12 but not other MBP-BTBs was able to pull down recombinant Sec13/31A.

(F) Sec31A is the direct binding partner for Klhl12. Sec31A and Sec13 were expressed separately in an in-vitro transcription/translation system, and incubated with MBP-BTBs coupled on amylose resins. Only Sec31A but not Sec13 was able to bind to MBP-Klhl12.

A

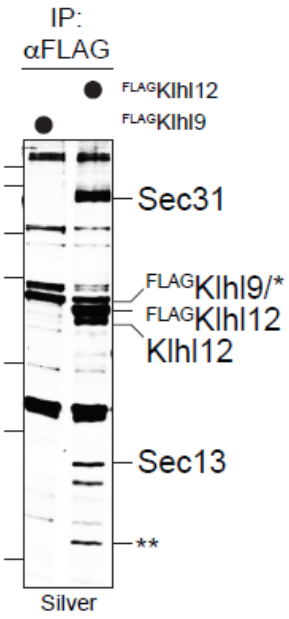
IP:
αFLAG
FLAGKlhl12
FLAGKlhl9
Sec31
FLAGKlhl9/*
FLAGKlhl12
Klhl12
Sec13
**
Silver

B


IP: αFLAG
FLAGKlhl9
FLAGKlhl12
FLAGKBTBD8
Sec31
Sec13
FLAG
Western

C

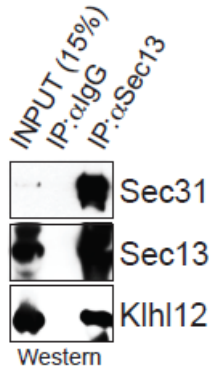
INPUT (15%)
IP:αIgG
IP:αSec13
Sec31
Sec13
Klhl12
Western

D

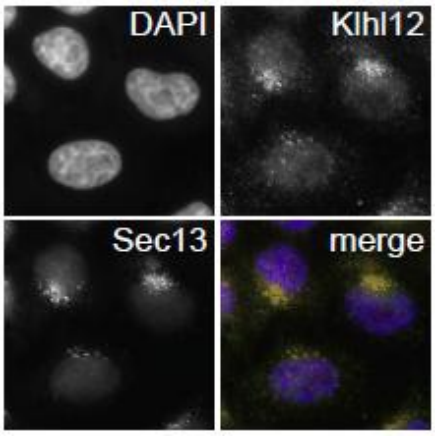
DAPI
Klhl12
Sec13
merge

E

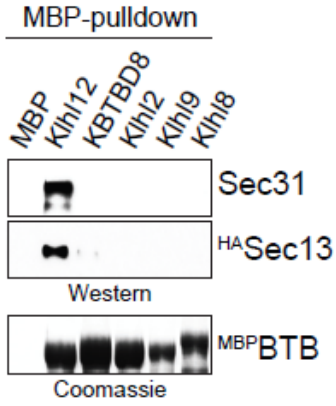
MBP-pulldown
MBP
Klhl12
KBTBD8
Klhl2
Klhl9
Klhl8
Sec31
HASec13
Western
MBPBTB
Coomassie

F

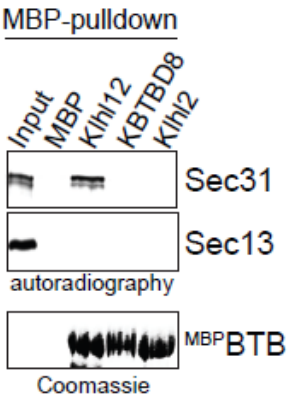
MBP-pulldown
Input
MBP
Klhl12
KBTBD8
Klhl2
Sec31
Sec13
autoradiography
MBPBTB
Coomassie

Fig. 4-2: Klhl12 interacts with Sec31A through the Kelch domain

(A) Alignment of Klhl12 Kelch repeats. The sequences in the boxes represent the β1, β2, β3, β4 strands of each Kelch repeat. Residues in red are the conserved residues for Kelch domain. The underlined sequences represent the loop sequences linking β2/β3 strands, and β4/β1 strands. The alignment is based the crystal structures of human Klhl12 Kelch domain (2VPJ.pdb) and mouse KEAP1 (1X2J.pdb).

(B) Identification of Klhl12 mutants unable to bind Sec31A. Structure of Klhl12 Kelch repeats was viewed from the top (left panel, adapted from PDB id: 2VPJ) and residues involved in Sec31A binding are highlighted in red. MBP-tagged wildtype and mutant Klhl12 were tested for their ability to bind radiolabeled Sec31A and Cul3 in an in vitro MBP binding assay. $Klhl12^{FG289AA}$, $Klhl12^{RGL369AAA}$, $Klhl12^{YDG434AAA}$ and $Klhl12^{RCY510AAA}$ are defective in binding Sec31A but not Cul3 (right panel).

(C) Klhl12 binds to 370aa-390aa of Sec31A. Sec31A fragments expressed by IVT system were tested for their ability to bind MBP-Klhl12 in an in-vitro binding assay. $Sec31A^{1-390}$ but not $Sec31A^{1-370}$ is able to bind Klhl12, indicating 370aa-390aa of Sec31A is involved in Klhl12 binding.

A

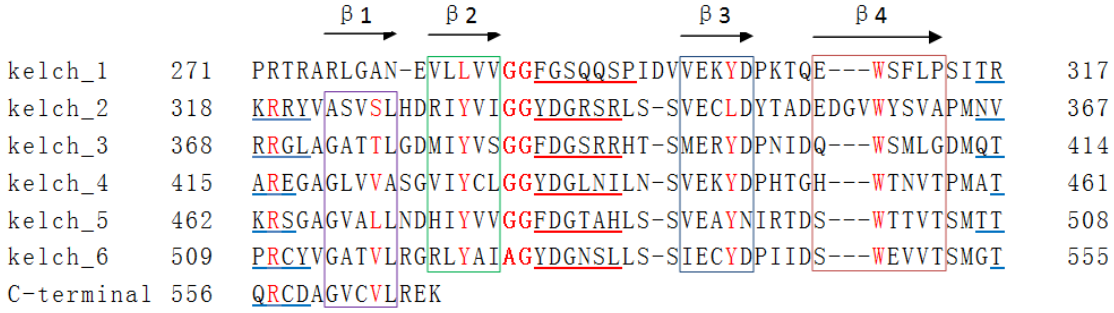
β 1
β 2
β 3
β 4
kelch_1 271 PRTRARLGAN-EVLLVVGGFGSQQSPIDVVEKYDPKTQE---WSFLPSITR 317
kelch_2 318 KRRYVASVSLHDRIYVIGGYDGRSRLS-SVECLDYTADEDGVWYSVAPMNV 367
kelch_3 368 RRGLAGATTLGDMIYVSGGFDGSRRHT-SMERYDPNIDQ---WSMLGDMQT 414
kelch_4 415 AREGAGLVVASGVIYCLGGYDGLNILN-SVEKYDPHTGH---WTNVTPMAT 461
kelch_5 462 KRSGAGVALLNDHIYVVGGFDGTAHLS-SVEAYNIRTDS---WTTVTSMTT 508
kelch_6 509 PRCYVGATVLRGRLYAIAGYDGNSLLS-SIECYDPIIDS---WEVVTSMGT 555
C-terminal 556 QRCDAGVCVLREK

B

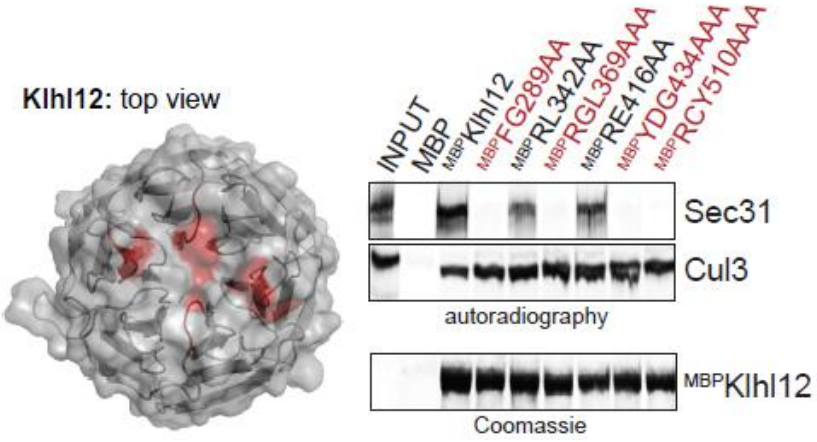
Klhl12: top view
INPUT
MBP
MBPKlhl12
MBPFG289AA
MBPRL342AA
MBPRGL369AAA
MBPRE416AA
MBPYDG434AAA
MBPRCY510AAA
Sec31
Cul3
autoradiography
MBPKlhl12
Coomassie

C

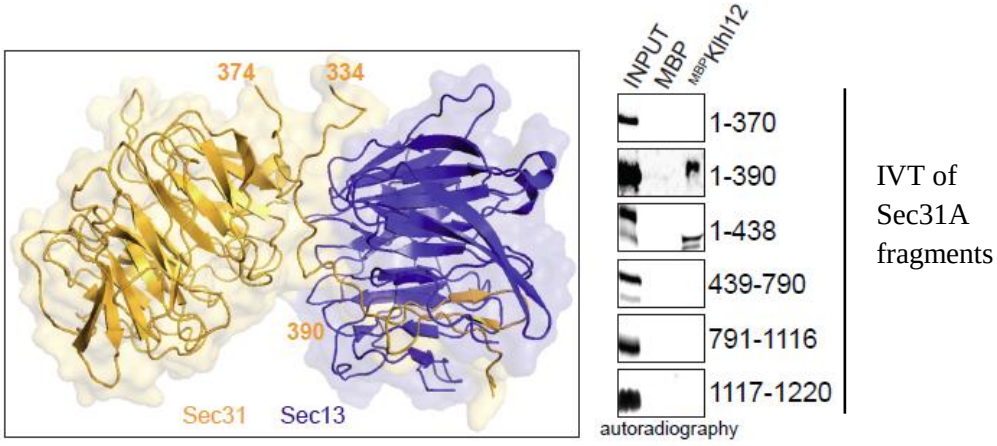
374
334
390
Sec31
Sec13
INPUT
MBP
MBPKlhl12
1-370
1-390
1-438
439-790
791-1116
1117-1220
autoradiography
IVT of Sec31A fragments

Fig. 4-3: Sec31A is mono-ubiquitinated by $Cul3^{Klhl12}$

(A) Purified Sec31A is mono-ubiquitinated by $Cul3^{Klhl12}$ in an in-vitro ubiquitination assay. Sec13/31A complex was used as the substrate and incubated with ubiquitination enzymes and untagged or His-tagged ubiquitin. Ubiquitination of Sec31A was determined by western blot.

(B) Sec31A ubiquitination is dependent on Klhl12 recognition. In-vitro ubiquitination of Sec31A was performed as in (A). Either wildtype or binding-deficient Klhl12 was added to the reaction, and ubiquitination of Sec31A was determined by western blot.

(C) Sec31A is mono-ubiquitinated in vivo. In-vivo ubiquitination of Sec31A was performed using a His-ubiquitin pulldown assay in 293T cells. Sec31A was expressed in the presence or absence of His-ubiquitin, Klhl12, wildtype or truncated Cul3 in 293T cells. Cells were lysed under denaturing conditions and ubiquitinated species were isolated by Ni-NTA IP. Ubiquitinated Sec31 was detected by western blot. Under physiological condition, Sec31A is mono-ubiquitinated (lane 2). Overexpression of Klhl12 and Cul3 induced the poly-ubiquitination of Sec31A (lane 3 & 4), which disappeared when a lysineless ubiquitin was expressed instead (lower two panels). Both mono- and poly-ubiquitination of Sec31A were abolished upon expression of truncated Cul3 (lane 5).

(D) Mono-ubiquitination of Sec31A in vivo is dependent on Cul3 and Klhl12. In-vivo ubiquitination of Sec31A by His-ubiquitin pulldown was performed as in (C). Endogenous Cul3 and Klhl12 were depleted by co-transfection of siRNA oligos with other plasmids in 293T cells.

(E) Binding-deficient Klhl12 mutants are unable to catalyze in-vivo ubiquitination of Sec31A. In-vivo ubiquitination of Sec31A by His-ubiquitin pulldown was performed as in (C) with the co-expression of wildtype and mutant Klhl12.

(F) Overexpression of Cul3 and Klhl12 causes Sec31A degradation in cells. Cul3 and different BTB genes were co-expressed in 293T cells. The endogenous level of Sec31A was detected by western blot.

(G) Endogenous levels of Cul3 and Klhl12 do not lead to Sec31A degradation. Hela cells were treated with siCul3, siKlhl12 or MG132 and protein level of Sec31A was detected by western blot.

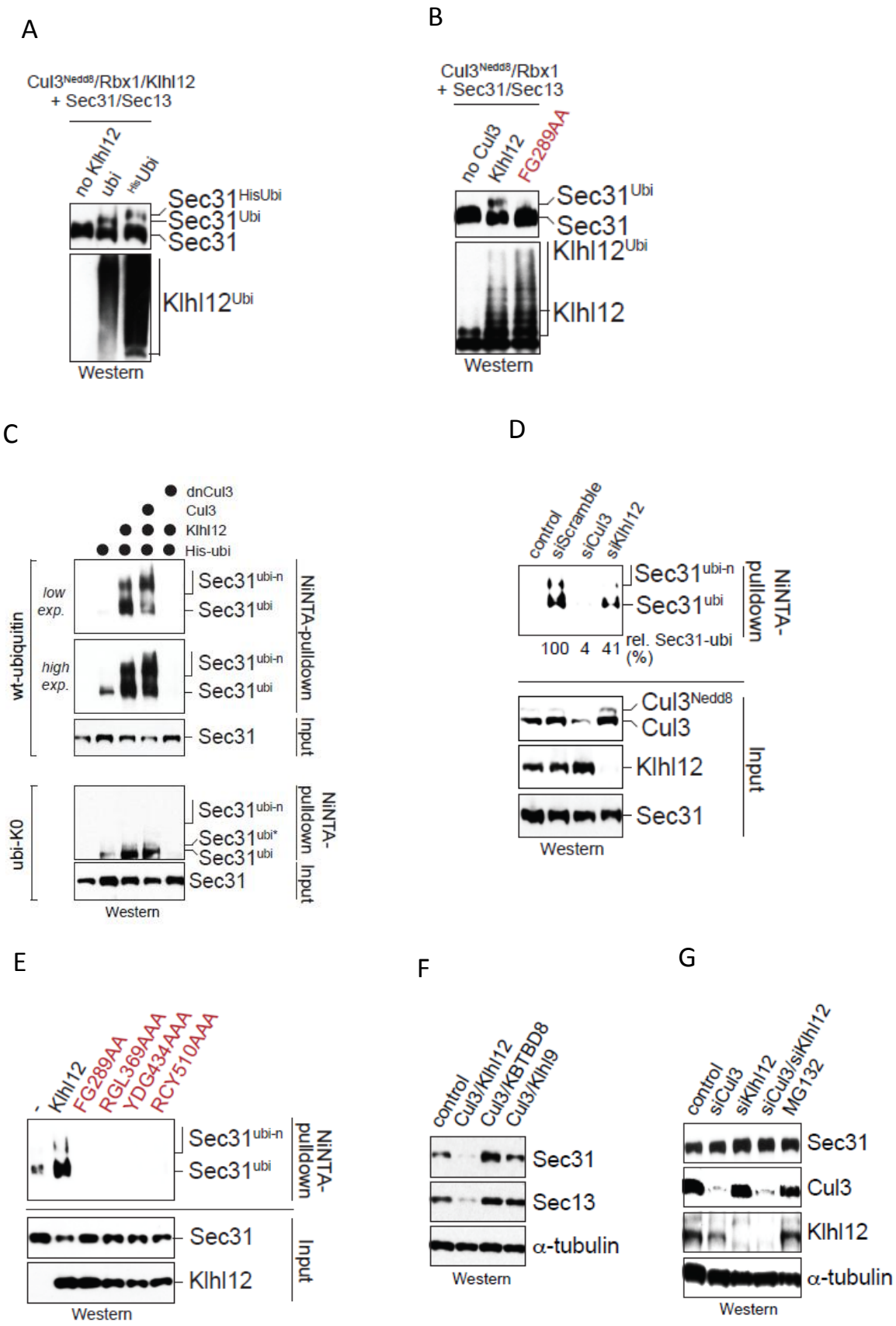
A
Cul3Nedd8/Rbx1/Klhl12
+ Sec31/Sec13
no Klhl12
ubi
HisUbi
Sec31HisUbi
Sec31Ubi
Sec31
Klhl12Ubi
Western
B
Cul3Nedd8/Rbx1
+ Sec31/Sec13
no Cul3
Klhl12
FG289AA
Sec31Ubi
Sec31
Klhl12Ubi
Klhl12
Western
C
dnCul3
Cul3
Klhl12
His-ubi
wt-ubiquitin
low exp.
high exp.
Sec31ubi-n
Sec31ubi
Sec31
NiNTA-pulldown
Input
ubi-K0
Sec31ubi*
Western
D
control
siScramble
siCul3
siKlhl12
Sec31ubi-n
Sec31ubi
NiNTA-pulldown
100 4 41
rel. Sec31-ubi (%)
Cul3Nedd8
Cul3
Klhl12
Sec31
Input
Western
E
-
Klhl12
FG289AA
RGL369AAA
YDG434AAA
RCY510AAA
Sec31ubi-n
Sec31ubi
NiNTA-pulldown
Sec31
Klhl12
Input
Western
F
control
Cul3/Klhl12
Cul3/KBTBD8
Cul3/Klhl9
Sec31
Sec13
α-tubulin
Western
G
control
siCul3
siKlhl12
siCul3/siKlhl12
MG132
Sec31
Cul3
Klhl12
α-tubulin
Western

Chapter Five

Ubiquitin-Dependent Regulation of COPII Coat Size and Function

5.1 Introduction

In the previous chapters, I have discussed the identification of $Cul3^{Klhl12}$ as an essential E3 ligase in mouse ES cells by regulating the Integrin-Src-Rac-Actin pathway. And the COPII coat protein Sec31A is the direct ubiquitination target for $Cul3^{Klhl12}$.

Typical COPII vesicles are approximately 60-80nm in diameter. However, some cell types secrete biological complex >300nm such as procollagen fibers and chylomicron (Fromme, et. al., 2005). Collagen is a group of naturally occurring proteins found mostly in the flesh and connective tissues of mammals. It is the major constituent of extracellular matrix (ECM) and plays an essential role in development by providing a scaffold for cell attachment and binding sites for plasma membrane receptors, such as integrins. The association of α / β -integrins with collagen initiates signaling events that regulate cell morphology, division, and differentiation. When the collagen export is compromised and a functional ECM is affected, integrins are removed from the plasma membrane by endocytosis, resulting in cell contraction and decreased proliferation. As a result, stem cells depend on collagen secretion for integrin-dependent cell division and survival.

Being synthesized as stiff triple-helical bundles of approximately 300nm long in the ER, procollagen fibers are secreted in a COPII-dependent manner upon hydroxylation of lysine and proline residues and further processed into collagen by enzymes in the ECM (Stephens, et. al., 2002). Compromised COPII function results in collagen deposition defects such as cranio-lenticulo-sutural dysplasia (CLSD) (Boyadjiev, et. al., 2006). It has long been a puzzle how COPII vesicle can adopt cargos like collagen, which is much larger than its normal size. Genetic screens for factors involved in protein secretion identified TANGO1, a collagen-specific COPII-adaptor (Saito, et. al., 2008). TANGO1 dimerizes with cTAGE5 at ER exit sites and interacts with collagen-VII and Sec23/24, the inner layer of a COPII coat (Saito, et. al., 2011). The deletion of TANGO1 in mice resulted in collagen deposition defects similar to those observed upon loss of COPII function. Germline mutations in the human TANGO1 homolog are associated with premature myocardial infarction, which is likely due to thinning of the collagen-cap of atherosclerotic plaques (Wilson, et. al., 2011). However, it is not known how the binding of TANGO1 to collagen change the geometry of COPII vesicle and increase its size.

In this chapter, I will discuss the observation that enhanced ubiquitination of Sec31A by $Cul3^{Klhl12}$ causes enlargement of COPII vesicle size in vivo by a still unknown mechanism. Consequently, $Cul3^{Klhl12}$ is required for collagen export in both embryonic stem cells and fibroblast cells, and subsequently the proper localization of integrins. My results have revealed the critical role of $Cul3^{Klhl12}$ in regulating embryonic stem cell proliferation and morphology by affecting COPII-dependent collagen export.

5.2 Results

5.2.1 $Cul3^{Klhl12}$ regulates the size of COPII coats

To study the biological function of mono-ubiquitination of Sec31A by $Cul3^{Klhl12}$, I induced Klhl12 expression in 293T stable cell line and followed the fate of Sec31A by microscopy. Three hours after induction, Klhl12 colocalized with endogenous Sec31A at small punctae of normal ER-exit sites (Fig. 5-1A). Overtime, these punctae grew into much bigger structures containing COPII components including Sec13 and Sec24C (Fig. 5-1B). The colocalization of Klhl12 with COPII components depends on the interaction between Klhl12 and Sec31 as depletion of Sec31 caused mislocalization of Klhl12 at 24 hours post induction (Fig. 5-1A). High-resolution microscopy shows that these structures are hollow and spherical, with a diameter of 200-500nm (Fig. 5-1C). Accordingly, both thin-section electron microscopy and immunogold EM revealed large, membrane-bound tubules in cells transfected with Klhl12 (Fig. 5-1D). The vesicles containing both Klhl12 and COPII components are possibly of ER origin and they do not contain components of either ERGIC, cis-Golgi or autophagosome (Fig. 5-1E).

The formation of these enlarged vesicles depends on ubiquitination by functional $Cul3^{Klhl12}$ as expression of dominant negative Cul3 or Klhl12 mutants that fail to recognize Sec31A abolishes the vesicle formation (Fig. 5-2A, 5-2B). Importantly, both wildtype ubiquitin and lysine-free ubiquitin colocalize with Sec31A in large vesicles upon Klhl12 expression, indicating that mono-ubiquitination of Sec31A by $Cul3^{Klhl12}$ is sufficient for vesicle formation (Fig. 5-2C). In fact, polyubiquitination of Sec31A by co-expression of both Cul3 and Klhl12 causes degradation of endogenous Sec31A at ER exit sites (Fig. 5-2A).

5.2.2 $Cul3^{Klhl12}$ promotes collagen transport from ER

Collagen is the major constituent of extracellular matrix (ECM) and provides a scaffold for cell attachment. It is synthesized as triple-helical procollagen fibers with a diameter of >300nm. In the presence of ascorbic acid, the proline and lysine residues of the procollagen fiber undergo hydroxylation which leads to its proper folding and subsequent secretion from ER in a COPII-dependent manner. It is not known yet how the typical COPII vesicle with a diameter of 60-80nm could accommodate a cargo much larger than itself. The observation that Klhl12 expression causes the formation of large vesicles containing COPII components suggests that ubiquitination by $Cul3^{Klhl12}$ could be involved in transport of big cargos like collagen.

To test this hypothesis, we expressed Klhl12 in IMR90 human fibroblasts and observed the localization of endogenous Collagen I by microscopy. This cell line produces a large amount of Collagen I which is blocked in ER due to deficiency of ascorbic acid in normal medium. However, in cells transfected with wildtype Klhl12, we saw the formation of big Klhl12-containing vesicles and that Collagen I was absent from ER. Notably, Collagen I re-accumulated in ER when brefaldin A (BFA) which blocks ER to Golgi transport was added to the media or the trace amount of ascorbic acid in the media was removed by dialysis (Fig. 5-3A). In contrast, adding either chloroquine to inhibit autophagy or MG132 to inhibit proteasomal degradation does not affect Collagen I localization upon Klhl12 expression. Cells expressing mutant Klhl12 or KEAP1, another BTB protein, still retain Collagen I in the ER. Meanwhile, Collagen I was found in the culture medium of Klhl12-expressing cells but not control cells by western blot (Fig. 5-3B). Our data indicate that Klhl12 expression indeed promotes Collagen transport from ER to Golgi and secretion.

To test whether endogenous Klhl12 and Cul3 are required for Collagen transport, we used the HT1080 fibrosarcoma cells stably expressing Collagen I. These cells secrete Collagen I even in normal medium containing low amount of ascorbic acid. However, when endogenous Cul3 or Klhl12 was depleted by shRNA, Collagen I was re-accumulated in ER (Fig. 5-3C). In contrast, depletion of Cul3 did not affect the localization of fibronectin, another component of ECM, or EGFR, a membrane protein whose localization also depends on transport from ER (Fig. 5-3D). We conclude that $Cul3^{Klhl12}$ is specifically required for transport of large cargos like Collagen but not small cargos.

5.2.3 $Cul3^{Klhl12}$ is required for attachment of ES cells to ECM

We have previously identified $Cul3^{Klhl12}$ as an important E3 ligase for embryonic stem cell morphology by regulating integrin-src-actin pathway. The fact that $Cul3^{Klhl12}$ is involved in COPII-dependent transport of large cargos from ER indicates that $Cul3^{Klhl12}$ may regulate the cellular attachment of ES cells by affecting the deposition of Collagen in ECM. To test this hypothesis, we depleted Cul3 or Sec13 as control in mouse ES cells and observed the localization of Collagen IV by microscopy. Collagen IV is a major component of ECM secreted by ES cells. The depletion of Cul3 or Sec13 by siRNA caused cellular accumulation of Collagen IV as well as the cell compaction phenotype (Fig. 5-4A). To confirm that the morphological change of Cul3 knockdown in ES cells is a direct consequence of Collagen transport defect, I coated the cell culture dish with either matrigel or Collagen IV, which rescued the Cul3 phenotype and restored integrin localization on plasma membrane (Fig. 5-4B). Together, our data show that $Cul3^{Klhl12}$ plays a key role in cell adhesion of ES cells by regulating COPII-dependent transport of Collagen.

5.3 Discussion

Collagen is the most abundant protein for mammals. It is found in many places throughout the body, such as skin, bone, organ and cartilage. Defects of COPII-dependent collagen secretion may cause severe genetic diseases including craniolenticulo-sutural dysplasia (CLSD). In vitro biochemical reconstitution and structural analysis have shown that the COPII coat protein Sec13/31A can spontaneously oligomerize to form a cuboctahedral cage with a diameter of 60~80nm. It has been a puzzle for a long time how the 300nm-long procollagen fibers are packed into COPII vesicles. In vitro experiments further suggested that Sec13/31A can form alternative geometrical structures (Stagg, et. al., 2008). How the flexibility in the size of COPII vesicles is regulated in vivo is not fully understood. Our finding that mono-ubiquitination of Sec31A by $Cul3^{Klhl12}$ causes enlarged COPII vesicles in cells shed light on the question. However, the detailed mechanism still remains to be studied. To prove that ubiquitination of Sec31A by $Cul3^{Klhl12}$ directly regulates the size of COPII vesicles and collagen transport, in-vitro COPII budding assay using purified COPII components can be established in the presence or absence of Cul3 and Klhl12. The efficiency of collagen transport can be

determined by western blot and the size of COPII vesicles can be measured by light scattering experiment. Given the fact that only a small fraction of Sec31 is ubiquitinated, it is more likely that the ubiquitin on Sec31A serves as a signal or binding site for a partner protein rather than playing a structural role. One possibility is that by interacting with collagen-specific receptors, ubiquitination of Sec31A stabilizes the COPII coat in assembly and delays the budding of COPII vesicle, leading to its enlargement. TANGO1, for example, consists of a transmembrane domain and an RGD domain which recognizes Collagen VII (Saito et. al., 2008). However, TANGO1 is not required for the budding of Collagen I. To identify additional collagen receptors, a stable cell line expressing epitope-tagged Collagen I can be established and its interacting proteins will be identified using biochemical methods and mass spec analysis. Potential binding partners for ubiquitinated Sec31A will be further isolated by identifying the transmembrane domain and ubiquitin binding motifs among the candidate proteins. Alternatively, the large vesicles induced by Klhl12 expression can be isolated by fractionation of cellular extract and differential centrifugation. Potential binding partners for ubiquitinated Sec31A can be subsequently identified by mass spec analysis. Finding the ubiquitination site on Sec31A may also help us to understand the function of ubiquitination. Mutagenesis screen of lysine to arginine on Sec31A did not yield a single mutant that failed to be ubiquitinated, indicating that the exact ubiquitination site might be flexible too. We can isolate the ubiquitinated Sec31A from the in-vitro ubiquitination assay and identify the favorable ubiquitination site by mass spec. Another question remains to be answered is how the ubiquitination is spatially and timely regulated. It is possible that a specific deubiquitinating enzyme (DUB) antagonizes the effect of $Cul3^{Klhl12}$ and Sec31A ubiquitination only happens when needed. Further biochemical analysis is needed to reveal the missing players.

5.4 Material and Methods

Analysis of collagen export from cells

IMR-90 human lung fibroblasts grown on 100mm dishes in DMEM/10% FBS were transfected with wt-Klhl12-flag, $Klhl12^{FG289AA}$-flag, Keap1-flag and pcDNA5-flag using nucleofection kit R (bought from Lonza) as described in manufacturer's protocol and plated on 6 well plate with 25mm coverslips. Dialyzed 10% FBS media was used for ascorbate free transfections. Brefeldin A (Sigma) was used at a concentration of 2.5mg/ml and cells were incubated for 30 minutes. MG132 was used at a concentration of 20 µ M and cells were incubated for 2 hours, choloroquine was used at a concentration of 200 µ M for 1 hour. Media was collected next day and cells on coverslips were fixed with 3% paraformaldehyde for 30 minutes and remaining cells on plate were used to prepare lysates. Cells on coverslips were permebealized with 0.1% Triton for 15 minutes at room temperature followed by blocking with 1% BSA for 30 minutes. Primary antibodies used were polyclonal anti Procollagen (LF-67,diluted 1:1000) and anti-flag (diluted 1:200). Secondary antibodies were Alexa fluor 546 donkey anti-rabbit IgG and Alexa Fluor 488 goat ant-rabbit IgG (diluted 1:200). After staining cells with appropriate primary and secondary antibodies, coverslips were fixed on slides using mounting reagent containing DAPI. Images were analyzed with a Zeiss Axio Observer Z1 fluorescent microscope and captured with Metamorph software (Molecular Devices). Merges of images were performed with ImageJ and LSM image Browser. Media collected from 6 well plate was normalized with respect to lysate

protein concentration estimated using BCA method. Media and lysates of each reaction were checked on western blot analysis. Tubulin was used as loading control for lysates.

A human fibrosarcoma cell line (HT1080) stably transfected with proalpha1(1) was used for Cul3 knockdowns. Cul3 shRNAs targeting two different regions were cloned into pSuperGFP and transfected using Lipofectamine 2000. pSuper GFP was used as negative control. Cells were grown on 25 mm coverslips in 6 well plate and fixed two days post transfection. Collagen staining was done using LF-67 (1:1000) and ER was stained with anti-PDI (1:1000) antibody. ER retention or secretion was scored in cells expressing GFP shRNAs. Cells without GFP shRNAs and transfected with pSUPER GFP were quantified as well. Lysates were prepared from remaining cells on 6 well and checked for knockdown efficiency.

Rescue experiment of Cul3-depleted mES cells by matrigel and Collagen IV

To rescue the phenotype of Cul3-depleted mES cells, TC dishes were coated with either growth factor reduced matrigel (BD Biosciences cat. # 356231) or purified collagen IV (BD Biosciences cat. # 354233) at 10 micrograms per cm2. Mouse ES cells treated with Cul3 siRNA were plated on top of the coated dishes.

Fig. 5-1: Klhl12 induces large vesicles with COPII coat

(A) Klhl12 expression induces formation of big punctae containing Sec31A during a time course. Trex 293T stable cell line was induced with doxycycline for Klhl12 expression for 3 hours, 5 hours and 24 hours. In one experiment, Cul3 was depleted by siRNA. The localization of $Klhl12^{FLAG}$ and endogenous Sec31A was visualized by immunofluoresence staining.

(B) The Klhl12-induced big punctae contain COPII components. Hela cells transiently transfected with $Klhl12^{FLAG}$ were subject to immunofluoresence staining using specific antibodies against FLAG and either of Sec31A, Sec13 and Sec24C. In one experiment, Sec31A was depleted by siRNA.

(C) High-resolution microscopy revealed that the Klhl12-induced big punctae are spherical and hollow structures containing COPII components. Hela cells transiently transfected with $Klhl12^{FLAG}$ and wildtype or lysineless ubiquitin were subject to immunofluoresence staining. Structures containing Klhl12 and COPII components were visualized by high-resolution confocal microscopy. In one experiment, Cul3 was depleted by siRNA.

(D) Thin section-EM (upper panels) and immunogold EM (lower panels) revealed the Klhl12-induced structures are double membrane-bound.

(E) The Klhl12-containing vesicles are not part of ERGIC, endosome, Golgi or autophagosome. Hela cells transiently transfected with $Klhl12^{FLAG}$ were subject to immunofluoresence staining using specific antibodies against FLAG and various subcellular markers.

A

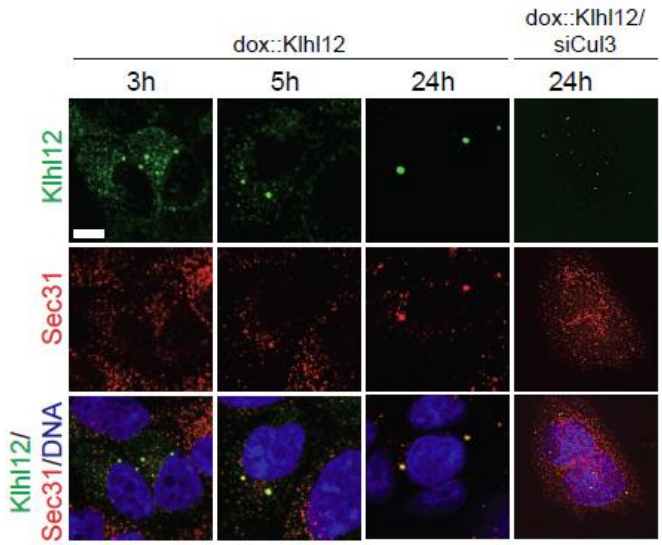
dox::Klhl12
dox::Klhl12/
siCul3
3h
5h
24h
24h
Klhl12
Sec31
Klhl12/
Sec31/DNA

B

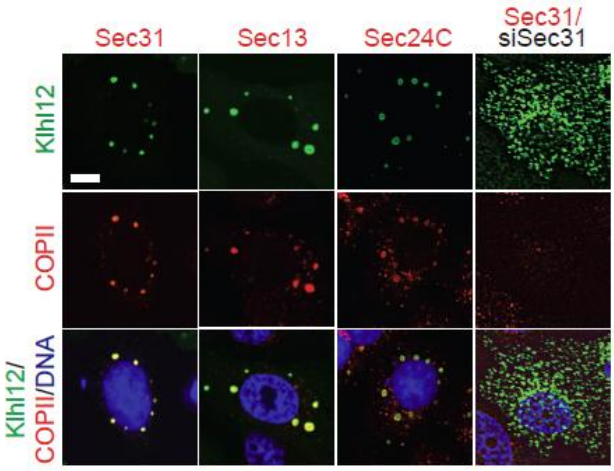
Sec31
Sec13
Sec24C
Sec31/
siSec31
Klhl12
COPII
Klhl12/
COPII/DNA

C

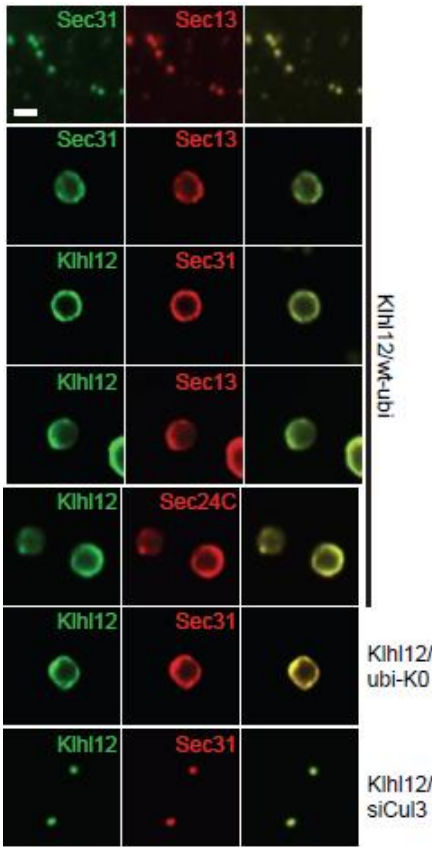
Sec31
Sec13
Sec31
Sec13
Klhl12
Sec31
Klhl12
Sec13
Klhl12/wt-ubi
Klhl12
Sec24C
Klhl12
Sec31
Klhl12/
ubi-K0
Klhl12
Sec31
Klhl12/
siCul3

D

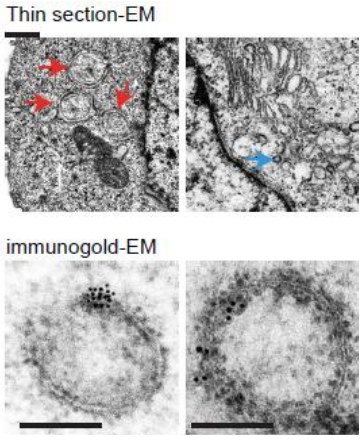
Thin section-EM
immunogold-EM

E

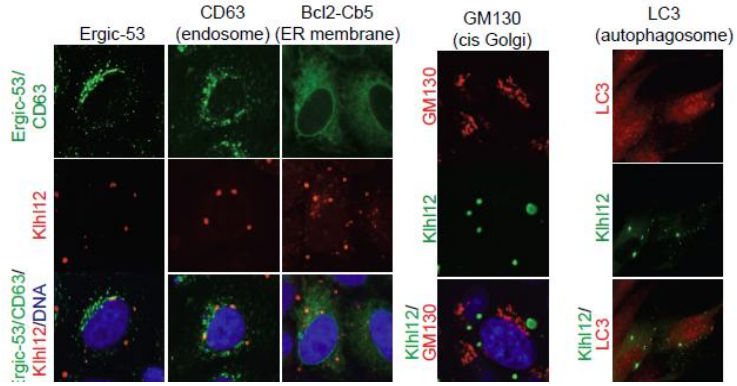
Ergic-53
CD63
(endosome)
Bcl2-Cb5
(ER membrane)
GM130
(cis Golgi)
LC3
(autophagosome)
Ergic-53/
CD63
Klhl12
Ergic-53/CD63/
Klhl12/DNA
GM130
Klhl12
Klhl12/
GM130
LC3
Klhl12
Klhl12/
LC3

Fig. 5-2: Formation of big vesicles upon Klhl12 expression is dependent on ubiquitination by $Cul3^{Klhl12}$

(A) Formation of big vesicles upon Klhl12 expression is dependent on functional Cul3 and Klhl12. Hela cells were transiently transfected with wildtype or mutant forms of Klhl12 and Cul3. The localization of Klhl12 and endogenous Sec31A was visualized by immunofluoresence staining.

(B) Klhl12 mutants that fail to bind Sec31A were unable to induce big vesicles containing COPII components. Hela cells were transfected with wildtype or mutant Klhl12 and subject to immunofluoresence staining against endogenous Sec31A.

(C) Monoubiquitination by $Cul3^{Klhl12}$ is sufficient for induction of big COPII vesicles. Hela cells were transfected with wildtype or lysineless ubiquitin in the presence or absence of Klhl12. Sec31A localization was analyzed by immunofluoresence staining.

A

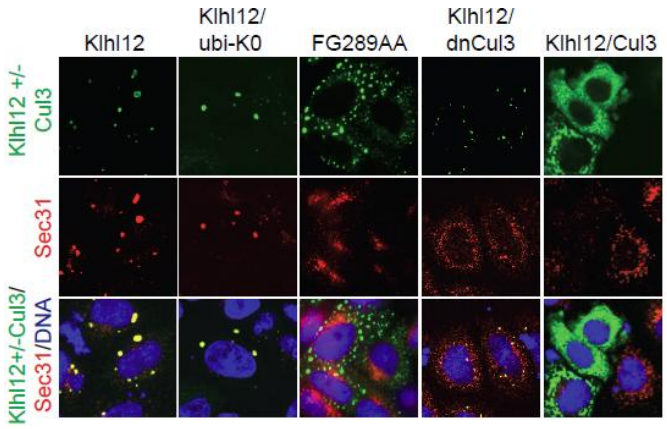
Klhl12
Klhl12/ ubi-K0
FG289AA
Klhl12/ dnCul3
Klhl12/Cul3
Klhl12 +/- Cul3
Sec31
Klhl12+/-Cul3/ Sec31/DNA

B

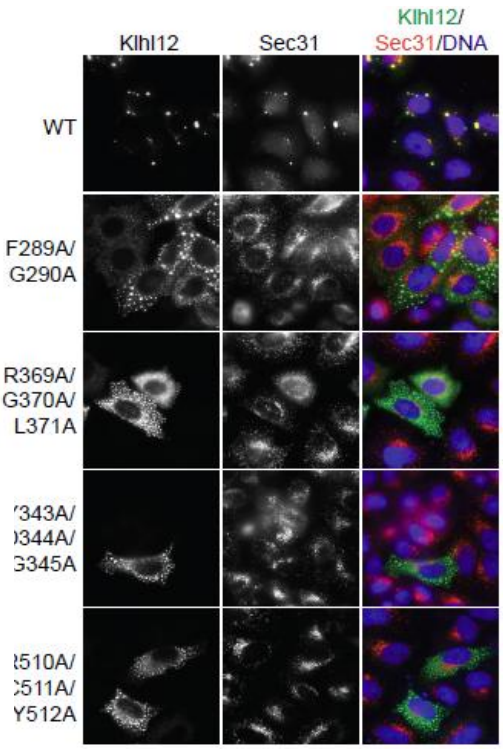
Klhl12
Sec31
Klhl12/ Sec31/DNA
WT
F289A/ G290A
R369A/ G370A/ L371A
'343A/)344A/ 3345A
:510A/ :511A/ Y512A

C

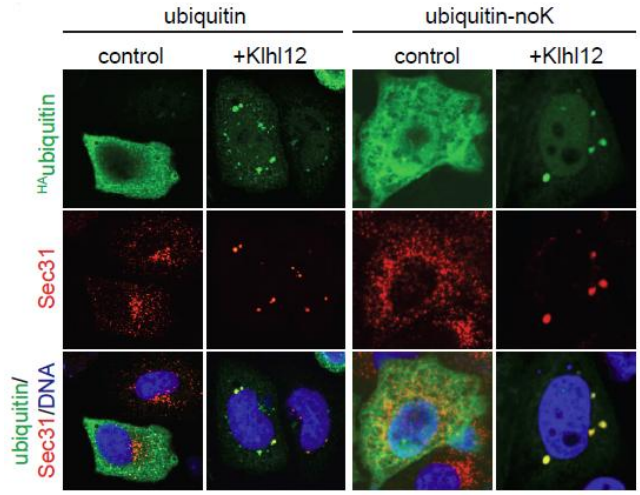
ubiquitin
ubiquitin-noK
control
+Klhl12
control
+Klhl12
HAubiquitin
Sec31
ubiquitin/ Sec31/DNA

Fig. 5-3: $Cul3^{Klhl12}$ is required for Collagen secretion from ER

(A) Klhl12 expression in IMR90 human fibroblasts promotes transport of Collagen I from ER. IMR90 cells were transiently transfected with either of Klhl12, $Klhl12^{FG289AA}$ or KEAP1 in the presence or absence of ascorbic acid or brefaldin A (BFA). The localization of Collagen I was analyzed by immunofluoresence staining (upper panel) and the percentage of transfected cells with secreted collagen is quantified as below (lower panel).

(B) Klhl12 expression in IMR90 human fibroblasts promotes secretion of Collagen I into the culture medium. IMR90 cells were transiently transfected with either of Klhl12, $Klhl12^{FG289AA}$ or control plasmids. Cellular lysate (L) and culture medium (M) were collected separately, and the level of Collagen I was determined by western blot. Tubulin was used as a control.

(C) Endogenous Cul3 and Klhl12 are required for Collagen I transport from ER. HT1080 human fibrosarcoma cells stably expressing Collagen I are transfected with pSuper-GFP shRNA constructs targeting either Cul3 or Klhl12. The localization of Collagen I was analyzed by immunofluorescence staining and PDI staining was used as an ER marker. The percentage of cells having Collagen I in ER was quantified as below.

(D) Endogenous Cul3 is not required for transport of fibronectin and EGFR from ER. Cul3 was depleted in HT1080 stable cell line by shRNA as described in (C). The localization of fibronectin and EGFR was analyzed by immunofluorescence staining. PDI staining was used as an ER marker.

A

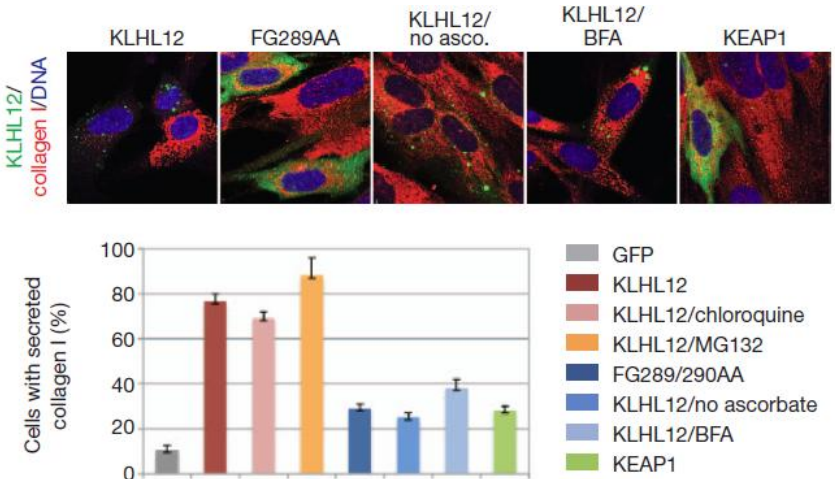
KLHL12
FG289AA
KLHL12/
no asco.
KLHL12/
BFA
KEAP1
KLHL12/
collagen I/DNA
Cells with secreted
collagen I (%)
100
80
60
40
20
0
GFP
KLHL12
KLHL12/chloroquine
KLHL12/MG132
FG289/290AA
KLHL12/no ascorbate
KLHL12/BFA
KEAP1

B

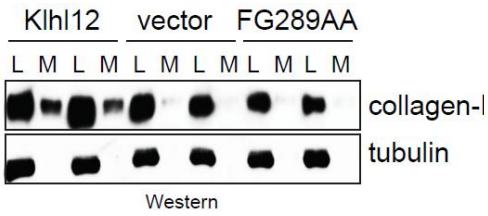
Klhl12
vector
FG289AA
L M L M L M L M L M L M
collagen-I
tubulin
Western

C

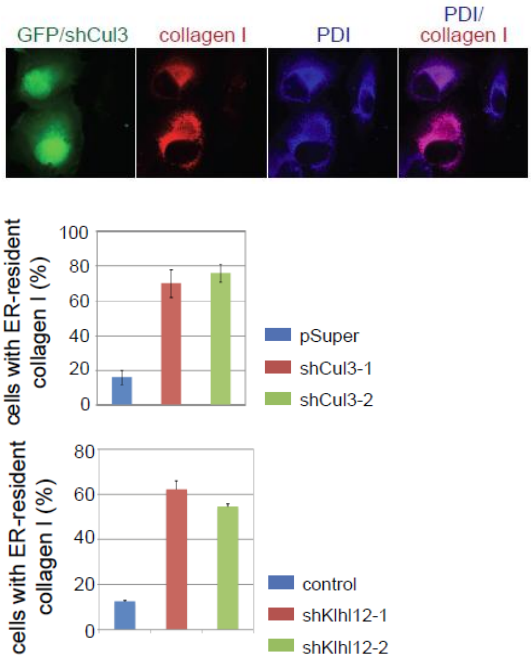
GFP/shCul3
collagen I
PDI
PDI/
collagen I
cells with ER-resident
collagen I (%)
100
80
60
40
20
0
pSuper
shCul3-1
shCul3-2
cells with ER-resident
collagen I (%)
80
60
40
20
0
control
shKlhl12-1
shKlhl12-2

D

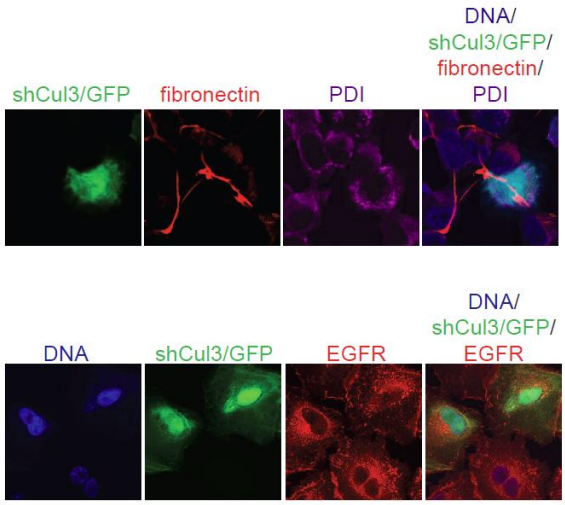
shCul3/GFP
fibronectin
PDI
DNA/
shCul3/GFP/
fibronectin/
PDI
DNA
shCul3/GFP
EGFR
DNA/
shCul3/GFP/
EGFR

Fig. 5-4: $Cul3^{Klhl12}$ regulates cell adhesion of mouse ES cells

(A) Cul3 is required for the secretion of Collagen IV in mouse ES cells. Cul3 or Sec13 was depleted by siRNA in mouse ES cells. Morphology of ES cell colonies was visualized by bright-field microscopy and the localization of Collagen IV was analyzed by immunofluoresence staining.

(B) Collagen IV rescues the morphological defect caused by Cul3 knockdown in mouse ES cells and restores integrin localization. Mouse ES cells depleted of Cul3 by siRNA were grown on surface coated with either gelatin, matrigel or purified Collagen IV. ES colonies were subject to immunofluoresence staining for actin and β1-integrin.

A

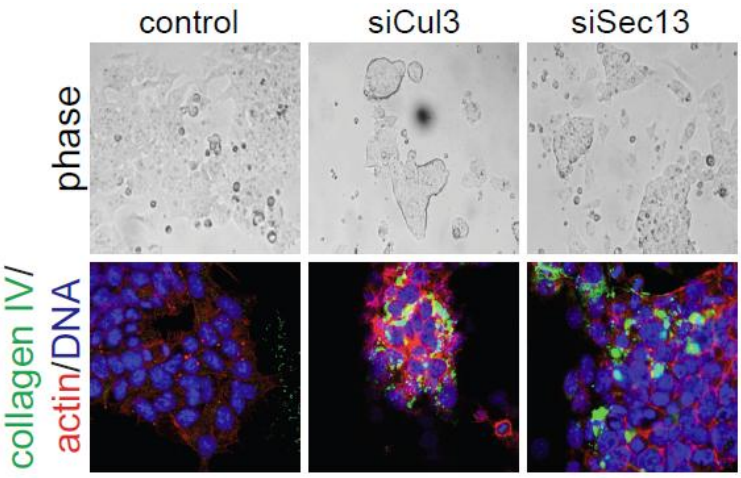
control
siCul3
siSec13
phase
collagen IV/
actin/DNA

B

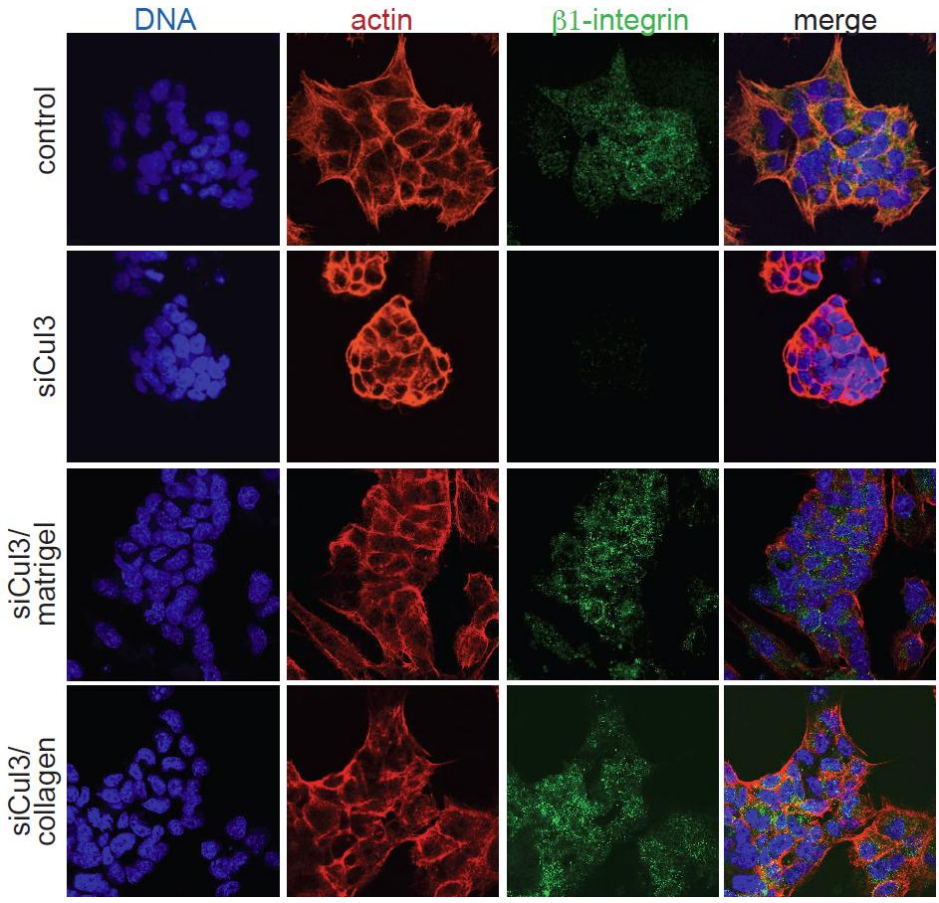
DNA
actin
β1-integrin
merge
control
siCul3
siCul3/
matrigel
siCul3/
collagen

REFERENCES

Adams, J., Kelso, R., & Cooley, L. (2000) The kelch repeat superfamily of proteins: propellers of cell function. *Trends in Cell Biol.* **10**, 17-24.

Angers, S., Thorpe, C.J., Biechele, T.L., Goldenberg, S.J., Zheng, N., MacCoss, M.J., & Moon, R.T. (2006) The KLHL12–Cullin-3 ubiquitin ligase negatively regulates the Wnt–β-catenin pathway by targeting Dishevelled for degradation. *Nat. Cell. Bio.* **8**, 348-357.

Aravind, L. & Koonin, E. V. (1999) Fold prediction and evolutionary analysis of the POZ domain: structural and evolutionary relationship with the potassium channel tetramerization domain. J. Mol. Biol. 285, 1353–1361.

Antonny B, Madden D, Hamamoto S, Orci L, Schekman R (2001) Dynamics of the COPII coat with GTP and stable analogues. *Nat Cell Biol*, **3**, 531-537.

Barlowe C, Schekman R (1993) SEC12 encodes a guanine-nucleotideexchange factor essential for transport vesicle budding from the ER. *Nature*, **365**, 347-349.

Bennett, E.J., Rush, J., Gygi, S.P., & Harper, W.J. (2010) Dynamics of Cullin-RING Ubiquitin Ligase Network Revealed by Systematic Quantitative Proteomics. *Cell*, **143**, 951-965.

Boyadjiev, S.A., Fromme, J.C., & et. al. (2006) Cranio-lenticulo-sutural dysplasia is caused by a SEC23A mutation leading to abnormal endoplasmic-reticulum-to-Golgi trafficking. *Nat Genet.* **38**, 1192-1197.

Bremm, A., Freund, S., & Komander, D. (2010) Lys11-linked ubiquitin chains adopt compact conformations and are preferentially hydrolyzed by deubiquitinase Cezanne. *Nat. Struc. & Mol. Biol.***17**, 939-948

Collins, T., Stone, J. R. &Williams, A. J. (2001) All in the family: the BTB/POZ, KRAB, and SCAN domains. Mol. Cell. Biol. 21, 3609–3615.

Fath, S., Mancias, J.D., Bi, X., & Goldberg, J. (2007) Structure and Organization of Coat Proteins in the COPII Cage. *Cell*, **129**, 1325-1336.

Fromme, J.C., & Schekman, R. (2005) COPII-coated vesicles: flexible enough for large cargo? *Curr. Opin. Cell. Biol.* **17**, 345-352.

Herzog, F., Primorac, I., Dube, P., Lenart, P., Sander, B., Mechtler, K., Stark, H., & Peters, JM, (2009) Structure of the Anaphase-Promoting Complex/Cyclosome interacting with a mitotic checkpoint complex. *Science*, **323**, 1477-1481

Jin, L., Williamson, A., Banerjee, S., Philipp, I., and Rape, M., (2008) Mechanism of ubiquitin-chain formation by the human anaphase-promoting complex. *Cell* **133**, 653-665.

Kirkpatrick, D.S., Hathaway, N.A., Hanna, J., Elsasser, S., Rush, J., Finley, D., King, R.W., and Gygi, S.P. (2006). Quantitative analysis of in vitro ubiquitinated cyclin B1 reveals complex chain topology. *Nat. Cell Biol.* **8**, 700–710.

Lasorella, A., Stegmuller, J., Guardavaccaro, D., Liu, G., Carro, M., Rothschild, G., Torre-Ubieta, L., Pagano, M., Bonni, A., & Iavarone, A. (2006) Degradation of Id2 by the anaphase-promoting complex couples cell cycle exit and axonal growth. *Natue*, **442**, 471-474.

Lederkremer GZ, Cheng Y, Petre BM, Vogan E, Springer S, Schekman R, Walz T, Kirchhausen T (2001) Structure of the Sec23p/24p and Sec13p/31p complexes of COPII. *Proc Natl Acad Sci USA*, **98**, 10704-10709.

Lee MC, Miller EA, Goldberg J, Orci L, Schekman R (2004) Bi-directional protein transport between the ER and Golgi. *Annu Rev Cell Dev Biol*, **20**, 87-123.

Martinez-Menarguez JA, Geuze HJ, Slot JW, Klumperman J. (1999) Vesicular tubular clusters between the ER and Golgi mediate concentration of soluble secretory proteins by exclusion from COPI-coated vesicles. *Cell*, **98**, 81-90.

McMahon, M., Thomas, N., Itoh, K., Yamamoto, M., & Hayes, J.D. (2006) Dimerization of Substrate Adaptors Can Facilitate Cullin-mediated Ubiquitylation of Proteins by a "Tethering" Mechanism. *Journ. Biol. Chem.* **281**, 24756-24768.

Presley JF, Cole NB, Schroer TA, Hirschberg K, Zaal KJ, Lippincott-Schwartz J (1997) ER-to-Golgi transport visualized in living cells. *Nature*, **389**, 81-85.

Rape, M., and Kirschner, M.W. (2004). Autonomous regulation of the anaphase-promoting complex couples mitosis to S-phase entry. *Nature* **432**, 588–595.

Reavie, L, Gatta, G.D., Crusio, K., & et. al. (2010) Regulation of hematopoietic stem cell differentiation by a single ubiquitin ligase–substrate complex. *Nat. Immu.* **11**, 207-217.

Reddy, S.K., Rape, M., and Kirschner, M.W. (2007). Ubiquitination by the anaphase-promoting complex drives spindle checkpoint inactivation. Nature 446, 921–925.

Saito, K., & et. al. (2008) TANGO1 Facilitates Cargo Loading at Endoplasmic Reticulum Exit Sites. *Cell*, **136**, 891-902.

Saito, K., Yamashiro, K., Ichikawa, Y., Erlmann, P., Kontani, K., Malhotra, V., & Katada, T. (2011) cTAGE5 mediates collagen secretion through interaction with TANGO1 at endoplasmic reticulum exit sites. *Mol. Biol. Cell.* **22**, 2301-2308.

Sato K, Nakano A (2005) Dissection of COPII subunit–cargo assembly and disassembly kinetics during Sar1p–GTP hydrolysis. *Nat Struct Mol Biol*, **12**, 167-174.

Sato, Y., Yoshikawa, A., Yamashita, M., Yamagata, A., & Fukai, S. (2009) Structural basis for specific recognition of Lys63-linked polyubiquitin chains by NZF domains of TAB2 and TAB3. *EMBO J.* **28**, 3903-3909.

Scales SJ, Pepperkok R, Kreis TE (1997) Visualization of ER-to-Golgi transport in living cells reveals a sequential mode of action for COPII and COPI. *Cell*, **90**, 1137-1148.

Schreiber, A., Stengel, F., Zhang, Z., Enchev, R., Kong, E., Morris, E., Robinson, C., Fonseca, P., & Barford, D. (2010) Structural basis for the subunit assembly of the anaphase-promoting complex. *Nature,* 470, 227-235.

Schulman, B. A. et al. (2000) Insights into SCF ubiquitin ligases from the structure of the Skp1–Skp2 complex. *Nature*. **408**, 381–386.

Singer, J.D., Gurian-West, M., Clurman, B., & Roberts, J.M. (1999) Cullin-3 targets cyclin E for ubiquitination and controls S phase in mammalian cells. *Gen. &. Dev.* **13**, 2375-2387

Song, L., & Rape, M., (2010) Regulated degradation of spindle assembly factors by the anaphase-promoting complex. *Mol. Cell* **38**, 369-382.

Stagg, S.M., Gurkan, C., Fowler, D.M., LaPointe, P., Foss, T.R., Potter, C.S., Bridget, C., & Balch, W.E. (2006) Structure of the Sec13/31 COPII coat cage. *Nature*, **439**, 234-238.

Stagg, S.M., Lapointe, P., Razvi, A., Gurkan, C., Potter, C.S., Carragher, B., & Balch, W.E. (2008) Structural Basis for Cargo Regulation of COPII Coat Assembly. *Cell*, **134**, 474-484.

Stegmeier, F., Rape, M., Draviam, V.M., Nalepa, G., Sowa, M.E., Ang, X.L., McDonald, E.R., 3rd, Li, M.Z., Hannon, G.J., Sorger, P.K., et al. (2007). Anaphase initiation is regulated by antagonistic ubiquitination and deubiquitination activities. *Nature*, **446**, 876–881.

Stephens, D.J., & Pepperkok, R. (2002) Imaging of procollagen transport reveals COPI-dependent cargo sorting during ER-to-Golgi transport in mammalian cells. *Journ. Cell. Sci.* **115**, 1149-1160.

Sumara, I., Quadroni, M., Frei, C., Olma, M.H., Sumara, G., Ricci, R., & Peter, M. (2007). A Cul3-Based E3 Ligase Removes Aurora B from Mitotic Chromosomes,Regulating Mitotic Progression and Completion of Cytokinesis in Human Cells. *Dev. Cell*, 12, 887-900.

Szutorisz, H., Georgiou, A., Tora, L., and Dillon N. (2006). The Proteasome Restricts Permissive Transcription at Tissue-Specific Gene Loci in Embryonic Stem Cell. Cell *127*, 1375-1388.

Thompson, B.J., Silvis, B., Sulis, M.L., & et. al., (2007). The SCF^{FBW7} ubiquitin ligase complex as a tumor suppressor in T cell leukemia. *Journal of experimental medicine*, **204**, 1825-2835.

Tong, K.I., Katoh, Y., Kusunoki, H., Itoh, K., Tanaka, T., & Yamamoto, M. (2006) Keap1 Recruits Neh2 through Binding to ETGE and DLG Motifs: Characterization of the Two-Site Molecular Recognition Model. *Mol. Cel. Biol.* **26**, 2887-2900.

Varadan, R., Assfalg, M., Haririnia, A., Raasi, S., Pickart, C., and Fushman, D. (2004) Solution conformation of Lys63-linked diubiquitin chain provides clues to functional diversity of polyubiquitin signaling. *J. Biol. Chem.* **279**, 7055-7063

Varadan, R., Assfalg, M., Raasi, S., Pickart, C., and Fushman, D. (2005) Structural determinants for selective recognition of a Lys48-linked polyubiquitin chain by a UBA domain. *Mol. Cell*. **18**, 687-698

Westbrook, T.F., Hu, G., Ang, X.L., Mulligan, P., Pavlova, N., Liang, A., Leng, Y., Maehr, R., Shi, Y., Harper, W.J., & Elledge, S.J. (2008) $SCF^{b\text{-}TRCP}$ controls oncogenic transformation and neural differentiation through REST degradation. *Nature*, **452**, 370-375.

Williamson, A., Banerjee, S., Zhu, X., Philipp, I., Iavarone, AT, & Rape, M. (2011), Regulation of ubiquitin chain initiation to control the timing of substrate degradation. *Mol. Cell* **42**, 744-757

Williamson, A., Jin, L., and Rape, M., (2009) Preparation of synchronized human cell extracts to study protein ubiquitination and degradation. *Methods Mol Biol.* **545**, 301-312.

Williamson, A., Wickliffe, K.E., Mellone, B.G., Song, L., Karpen, G.H., & Rape, M. (2009) Identification of a physiological E2 module for the human anaphase-promoting complex. *Proc Natl Acad Sci U S A*, **106**, 18213-18218.

Wilson, D.G., & et. al. (2011) Global defects in collagen secretion in a Mia3/TANGO1 knockout mouse. *Journ. Cell. Biol.* **193**, 935-951.

Wickliffe, K.E., Lorenz, S., Wemmer, D.E., Kuriyan, J., & Rape, M. (2011) The mechanism of linkage-specific ubiquitin chain elongation by a single-subunit E2. *Cell*, **144**, 769-781

Wickliffe, K.E., Williamson, A., Jin, L., and Rape M., (2009) The multiple layers of ubiquitin-dependent cell cycle control. *Chem Rev.* **109**, 1537-1548.

Xu, L., Wei, Y., Reboul, J., Vaglio, P., Shin, T., Vidal, M., Elledge, S.J., & Harper, W.J. (2003) BTB proteins are substrate-specific adaptors in an SCF-like modular ubiquitin ligase containing CUL-3. *Nature*, **425**, 316-321.

Yoshihisa T, Barlowe C, Schekman R (1993) Requirement for a GTPase-activating protein in vesicle budding from the endoplasmic reticulum. *Science*, **259,** 1466-1468.

Zheng, N. et al. Structure of the Cul1-Rbx1-Skp1-F boxSkp2 SCF ubiquitin ligase complex. (2002) *Nature*,**416**, 703–709.

Zhuang, M., Calabrese, M.F., Liu, J., & et. al., (2009) Structures of SPOP-Substrate Complexes: Insights into Molecular Architectures of BTB-Cul3 Ubiquitin Ligases. *Mol. Cell.* **36**, 39-50.

Zimmerman, E.S., Schulman, B.A., & Zheng, N. (2010) Structural assembly of cullin-RING ubiquitin ligase complexes. *Curr. Opin. In. Struc. Biol.* **20**, 714-721